High-energy nucleon–nucleon scattering

N. Hoshizaki
University of Kyoto, Kyoto, Japan
Fiz. Él. Chast. Atom. Yad., 4, 79-126 (January-March 1973)

The methods and results of phase-shift analysis of high-energy nucleon–nucleon scattering (between 400 MeV and 3 GeV) are described. There is a discussion of physical results concerning repulsive cores in the singlet and triplet even-parity states of the nucleon–nucleon system, nonstatic effects of higher order in L in the triplet odd-parity state, and the peripheral nature of absorption processes.*

1. INTRODUCTION

High-energy nucleon–nucleon scattering (at $E \gtrsim 400$ MeV) is an important source of detailed information about nuclear forces at the shortest ranges (in "region III"). Here we will review the most recent progress in the phenomenological study of this scattering (by means of phase-shift analysis). The analytic methods are discussed in some detail, and the most recent physical results are reported. We will be concerned primarily with energies between 400 MeV and a few GeV. We will briefly discuss scattering at higher energies, in connection with a discussion of the phase-shift results at lower energies.

Until recently phase-shift analysis was carried out only below 400 MeV. Attempts to extend the analysis to higher energies ran into several difficulties: Diffraction effects due to pion creation had to be taken into account; it was expected that a large number of partial waves would contribute to the scattering; there were important gaps in the experimental information, so this information could not be analyzed without a reliable theory, etc. An analytic method has been designed to cope with these difficulties:[1,2]

1) The imaginary parts of the phase shifts are evaluated on the basis of pion-production data with the help of the resonance model for pion production.[3]

2) The real parts of the phase shifts are determined through extrapolation of the well–known phase-shift solutions for energies below 400 MeV.

This method was first used successfully to analyze data on p–p scattering at[2,4] 660 MeV, and it was used subsequently for[5] 1 GeV. The 660-MeV results were also analyzed independently at Dubna[6] with restriction 1). Recent analyses carried out at Dubna, Kyoto, and Livermore have now led to a qualitative determination of the phase shifts for p–p scattering at energies up to 700 MeV within the restrictions stated above.

To extend the analysis above 1 GeV, we should modify restriction 1, since in this energy range the Mandelstam model is less valid. An early approach was as follows:[7]

1') The L dependence of the imaginary parts of the phase shifts was inferred from the results of the phase-shift analysis for energies below 1 GeV. Furthermore, in an effort to reduce the increasing number of free parameters, it was necessary to impose the following requirement, which follows from theory:

3) The nuclear forces are described by a one-boson exchange mechanism at intermediate and long ranges.[8] Analysis of data at 1, 2, and 3 GeV has largely supported this approach.[7,9]

The imaginary parts of the phase shifts were recently calculated on the basis of the one-pion-exchange model for pion production, through the use of unitarity.[10] This model is valid for energies of about 1 GeV, so it can be used to supplement the Mandelstam model. Critical analysis shows that restriction 1) should be replaced by the following restriction:[11]

1") The imaginary parts of the phase shifts corresponding to L above a certain critical value are described correctly by a one-pion-exchange model.[10]

The most reliable method currently available for analyzing data near 1 GeV is based on the use of restrictions 1"), 2), and 3); this method has been used successfully to analyze data on p–p scattering at[11] 970 MeV. The one-pion-exchange model has been used independently to analyze data on p–p scattering at[12] 660 MeV.

The phase shifts for nucleon–nucleon scattering above 3 GeV are still unknown. The only results available are based on an analysis of their possible asymptotic behavior and the assumption that the interaction is independent of the spin in the asymptotic energy range.[13,13a]

Restrictions 1") and 3) are based on the general principle of ref. 14, which is apparently valid as we move from the outer part of the nucleon to the inner part, combining our faith in the theoretical description of the outer part of the nucleon with a phenomenological description of its inner part. According to this principle, scattering and absorption near the edge of the nucleon are treated on the basis of pion theory.

It is currently believed that the nuclear forces at long ranges ($x \gtrsim 1.5\hbar/\mu_\pi c$, where x is the distance between particles) are governed by one-pion exchange,[15] while in the intermediate range ($0.5\hbar/\mu_\pi c \lesssim x \lesssim 1.5\hbar/\mu_\pi c$) they are governed primarily by the exchange of several heavy mesons of various types and masses (the one-boson-exchange model).[8] Particles incident with large impact parameters and thus large angular momenta are affected only by the long-range part of the force. The phase shifts for states having L above a critical value can be determined from a one-boson-exchange model[7] incorporating one-pion exchange.[16]

This understanding of the outer part of the force range allows us to study the inner part (region III). This region has been treated only purely phenomenologically; the usual assumption is that there is a solid repulsive core,[17] as has been confirmed experimentally in the singlet even-parity state,[18] and perhaps in the triplet odd-parity state also. In a potential model which reproduces the experimental phase shifts below 400 MeV it is assumed that the hard core is present in all states and has a radius[19] of $r_c \approx 0.5 \cdot 10^{-13}$ cm.

However, there is no physical basis for assuming that the hard core found in this manner actually represents some absolutely hard barrier; some softness should be taken into account. (The core is "hard" if the potential barrier is quite high and has a sharp profile, and it is "soft" if the forces are relatively weak and have a long tail.) In this case, how soft is the actual core? The existing data obtained below 400 MeV allow us to determine only a single parameter of the core (its radius). To answer this question we must thus analyze the behavior of the phase shifts of the lower-order partial waves at higher energies. This circumstance has furnished one of the motivations for phase-shift analysis at high energies.[1,2]

2. REVIEW OF THE PHASE SHIFTS IN NUCLEON–NUCLEON SCATTERING BELOW 400 MeV

Phase shifts for p–p scattering below 400 MeV. An unambiguous phase-shift solution is now available for all energies below 400 MeV. This solution was found in the following manner. The first complete measurements of p–p scattering at 310 MeV led to five sets of phase shifts,[18] whose number was subsequently reduced to two through a modified analysis[16] ("solutions 1 and 2"). In the modified analysis, in correspondence with the general principle,[14] the contributions to the scattering amplitude of the states having the higher angular momenta were evaluated on the basis of one-pion exchange. Modified analysis at 210 MeV also led to two corresponding solutions; finally, recent complete and accurate measurements at 145 and 50 MeV pointed to a single solution,[20] 1. Accordingly, if we assume that at large ranges the nuclear forces are governed by one-pion exchange and that the phase shifts vary smoothly as functions of the energy, we can conclude that the phase shifts for p–p scattering below 400 MeV can be represented unambiguously by solution 1. These phase shifts were reported in ref. 21. The basic properties of solution 1 can be understood on the basis of a discussion of the potential (see below).

Phase shifts for n – p scattering below 400 MeV. The successful determination of the p–p phase shifts facilitated derivation of an unambiguous matrix for n–p scattering. If we assume the nuclear forces to be charge-independent, we find the isotriplet part of the matrix for n–p scattering from the matrix for p–p scattering. As was mentioned above, this part of the matrix is now known, and we need only find information about the rest of the isosinglet part of the scattering matrix from data on n–p scattering. Then only three independent measurements are required for a complete determination of the isosinglet part over the entire angular range ($0 \leq \theta \leq \pi$). At present data on triple n–p scattering have been obtained for 95, 140, 210, MeV, etc. Combining the results of these measurements with data on the differential scattering cross sections and the polarization for each energy, we have essentially all the necessary information. Analyses based on charge independence have been carried out since 1961. If we adopt solution 1 for the isotriplet parts of the scattering matrices for various energies, we also find solutions of one and only one type for the isosinglet parts.[22] These phase shifts were reported in ref. 21.

Energy-dependent analysis. The analyses discussed above have been based on data for a single energy. Experimental data obtained for various energies can be analyzed simultaneously if a functional dependence of the scattering matrix on the energy is chosen in some appropriate manner. A typical example of such an analysis is an analysis based on a potential model; we describe the results of this analysis below. In other analyses of this type the phase shifts are written as energy-dependent functions containing adjustable parameters. In the early studies[23,24] the functional dependences used were purely mathematical or were physically unsatisfactory, although these analyses did make a contribution to the establishment of solution 1. These unsatisfactory functional dependences were improved in recent analyses at Livermore based on the requirements of the partial-wave dispersion relations.[25] The results of these analyses were reported in ref. 21.[1)]

Potential model. The basic features of the phase shifts for p–p and n–p scattering below 400 MeV can be understood on the basis of the following semiphenomenological potential model:

$$V = V(\mathrm{OPEP}) + V_{\mathrm{II}} + V(\text{ core }), \tag{1}$$

where V(OPEP) represents the one-pion-exchange potentials, V_{II} represents the phenomenological potentials, which become important in the intermediate range ($1.5\hbar/\mu_\pi c \gtrsim x \gtrsim 0.4\hbar/\mu_\pi c$), and V(core) represents the hard core of radius $r_c \approx 0.35\hbar/\mu_\pi c$ (see ref. 26 for more details).

In the outer region ($x \gtrsim 1.5\hbar/\mu_\pi c$) the contribution from V(OPEP) predominates, while in the intermediate region the sum V(OPEP) + V_{II} predominates. In this region V(OPEP) is primarily a weak attractive central part in the ^1E state,[2)] a relatively strong repulsive tensor part in the ^3O state, strong attractive central and tensor parts in the ^3E state, and a strong repulsive central part in the ^1O state. The potentials V_{II} are characterized by a strongly attractive LS part in the ^3O state; more precisely, V_{II} contains:

a strong attractive central part and a weak quadratic LS part	for the ^1E state; (2a)
weak central and tensor parts and a strong attractive LS part	for the ^3O state; (2b)
weak central and tensor parts and a weak LS and/or quadratic LS part	for the ^3E state; (2c)
a weak central part	for the ^1O state. (2d)

The nonstatic parts (LS and quadratic LS) of the ^3E state have still not been determined unambiguously because of the large errors involved in the experimental phase shifts of the ^3D states.

One-boson-exchange model. Potentials V_{II} described above have been studied on several occasions. It is now believed that these potentials are due primarily to one-boson exchange and uncorrelated two-pion exchange.[8] The minimum set of necessary heavy mesons is: 1) a vector boson with isospin 1 (which interacts with a nucleon primarily through tensor coupling); 2) a vector boson with isospin 0 (which interacts primarily through vector coupling); and 3) a scalar boson with isospin[27] 0. The first two mesons are easily identified as ρ and ω mesons, respectively. The third may be the hypothetical σ meson, which may or may not be necessary, depending on how weak the central parts of the potential for uncorrelated 2π exchange are.[27]

Another useful model, one of the simplest one-boson-exchange models, is the OBEC model, in which only the lower-order diagrams for one-boson exchange are taken into account in calculation of the phase shifts.[28] This calculation is simple and relativistically invariant, so this model can apparently be used at high energies. In phase analysis above 1 GeV the following set of parameters, obtained in an analysis of experimental data for energies[29] below 400 MeV, has been used:

$$g_v^2 = 11.0; \quad g_v f_v = 0.7; \quad f_v^2 = 0.04 \tag{3a}$$

for the coupling constant of the ω meson and the nucleon,

$$g_v^2 = 1.6; \quad g_v f_v = -3.2; \quad f_v^2 = 6.5 \tag{3b}$$

for the coupling constant of the ρ meson and the nucleon,

$$g_s^2 = 13.1 \tag{3c}$$

for the coupling constant for the scalar meson and the nucleon. Here g_V and f_V are the vector and tensor coupling constants, respectively. The mass of the scalar meson was assumed to be 500 MeV.

3. FORMULATION OF THE ANALYSIS METHOD FOR ENERGIES ABOVE 400 MeV

Analysis method between 400 MeV and 1 GeV. In principle, a complete reconstruction of the amplitude for p–p scattering without the use of any approximate assumptions requires 11 experiments. Current experimental studies have not yet satisfied this requirement, however, so any meaningful analysis must make use of certain physically plausible assumptions. Our analysis method, as mentioned in Sec. 1, is as follows:

1) The imaginary parts of the phase shifts are evaluated from data on pion production. In this energy range this evaluation is based on the resonance (3.3) model for pion production.

2) Since a single-valued phase-shift solution is available below 400 MeV, we began the analysis in the adjacent energy range (i.e., at 500–700 MeV). By extrapolating the solution found below 400 MeV we restrict the region in which we must seek the real parts of the phase shifts. If a plausible solution is found in this manner, we turn to an analysis in the next higher energy range (i.e., at 800–1000 MeV), again making use of the extrapolation procedure.

3) We assume that for the higher-order partial waves, which should be scattered in the outer part of the force range, the phase shifts can be represented in terms of a contribution of one-pion exchange.[16] The other phase shifts can be adjusted in phase-shift space, as described in 2), and they can be determined from experimental data by the method of least squares. For the phase shifts of states having intermediate angular momenta, qualitative use is made of the values predicted by the one-boson-exchange model.[29]

Parametrization of the scattering matrix. More specifically, the S matrix for elastic scattering is parametrized in the form

$$S_{LJ} = r_{LJ} \exp(2i\delta_{LJ}) \tag{4}$$

for the singlet and triplet unbound states, where δ are the real parts of the phase shifts and the quantities r are the absorption parameters. The quantity r_{LJ} is a real positive number less than unity, and the quantity $1 - r_{LJ}^2$ gives the relative part of the incident wave with given L, J which goes into inelastic channels. For the triplet bound state with $L = J \pm 1$, the S matrix is a nondiagonal 2×2 matrix. It is parametrized by an ambiguous method, which can be described by[11] (see Appendix 1)

$$S = \begin{bmatrix} S_{J-1,\,J} & R^J \\ R^J & S_{J+1,\,J} \end{bmatrix}, \tag{5}$$

where

$$S_{J\mp1,\,J} = [1 - (r_\pm / r_\mp)\,\rho_J^2]^{1/2}\, r_\mp \exp(2i\delta_\mp);$$
$$R^J = i\rho_J (r_- r_+)^{1/2} \exp[i(\delta_- + \delta_+ + \varphi_J)].$$

Here we have $r_\mp = r_{J\mp1,J}$ and $\delta_\mp = \delta_{J\mp1,J}$. The ρ_J reflect the mixing of the states with $L = J - 1$ and $J + 1$. When the energy falls below the threshold energy for inelastic scattering, all the inelastic parameters vanish ($r_{LJ} \to 1, \varphi_J \to 0$), and matrix (5), with $\rho_J = \sin 2\varepsilon_J$, assumes a form corresponding to the Stapp parametrization.[18] One advantage of parametrization (5) is that the quantity $1 - r_{LJ}^2$ has the same physical meaning in the singlet and triplet unbound states. Accordingly, the total reaction cross section for p–p collisions is described by

$$\sigma_r = \sigma_r(S) + \sigma_r(T); \tag{6}$$

$$\sigma_r(S) = \frac{1}{2}\pi\lambda^2 \sum_{\substack{J \\ (\text{even})}} (2J+1)\{1 - ({}^1r_J)^2\}; \tag{7}$$

$$\sigma_r(T) = \frac{1}{2}\pi\lambda^2 \sum_{\substack{J \\ (\text{odd})}} \sum_{L=|J-1|}^{J+1} (2J+1)\{1 - ({}^3r_{LJ})^2\}, \tag{8}$$

where probability conservation has been used. This parametrization is related to others in Appendix 1.

Absorption parameters. Restriction 1) can be formulated in the following manner. It is assumed in the resonance (3,3) model that the escaping pion is in a resonance state with one of the nucleons, with $I_{\pi N} = 3/2$ and $J_{\pi N} = 3/2$, where $I_{\pi N}$ and $J_{\pi N}$ are the isospin and angular momentum in the pion–nucleon subsystem. If the remaining nucleon is in the S state with respect to the center of mass of the entire system, pion production occurs by means of

$${}^1D_2 \to S(3,3) \tag{9}$$

because of conservation of parity and total angular momentum. Here (3,3) refers to the (3/2, 3/2) state mentioned above, formed by the pion and one of the nucleons with respect to the center of mass of the entire system. Transition (9) is called "production in the S state."[3)] Analogously, if the second escaping nucleon is in the P state with respect to the center of mass of the entire system, the following transitions occur (production in the P state):[4)]

$$\left.\begin{matrix} {}^3P_{0,1,2} \searrow \\ {}^3F_{2,3} \nearrow \end{matrix}\right. P(3,3), \qquad (10)$$

where the letter P in the final state refers to the angular-momentum state of the second nucleon with respect to the center of mass of the entire system. As the initial energy increases, we should supplement (9) and (10) by production in the D state:[5)]

$$\left.\begin{matrix} {}^1S_0 \searrow \\ {}^1D_2 \rightarrow \\ {}^1G_4 \nearrow \end{matrix}\right. D(3,3). \qquad (11)$$

We see from (9)-(11) that we have ${}^1r_J = 1$ for $J > 4$ and ${}^3r_{LJ} = 1$ for $J \geq 4$.

Transforming from the representation of the final three-particle system above to a representation in which two nucleons form a single subsystem, we find that the final states in transitions (9)-(11) are formed in the following manner:

$$S(3,3) \approx d\pi^+ \quad \text{or} \quad (np)_S\pi^+; \qquad (12)$$
$$P(3,3) \approx (np)_P\pi^+ \quad \text{or} \quad pp\pi^0; \qquad (13)$$
$$D(3,3) \approx (np)_D\pi^+. \qquad (14)$$

Here the subscripts denote the angular-momentum states of the escaping nucleons in the new subsystem. We note that in (13) the escaping protons in the $pp\pi^0$ system are always in the P state because of the Pauli principle.

Combining these results with (7), we find

$$\frac{1}{2}\pi\lambda^2 \sum_{\substack{J=0 \\ (\text{even})}}^{4} (2J+1)\{1-({}^1r_J)^2\} = \sigma(d\pi^+) + {}^1a\sigma(np\pi^+) \qquad (15)$$

for the singlet states, where

$${}^1a = \{\sigma((np)_S\pi^+) + \sigma((np)_D\pi^+)\}/\sigma(np\pi^+),$$

and $\sigma[(np)_S\pi^+]$ and $\sigma[(np)_D\pi^+]$ are the cross sections for the reactions $pp \rightarrow (np)_S\pi^+$ and $pp \rightarrow (np)_D\pi^+$, respectively.

Production in the D state, (11), can be neglected[3] up to 660 MeV. In this case we have ${}^1r_0 = {}^1r_4 = 1$, and ${}^1r_2$ is determined by substituting the experimental cross section into the right-hand side of Eq. (15).[30] Above 660 MeV production in the D state must also be taken into account. In this case two of the parameters ${}^1r_J$ must be determined, along with the real parts of the phase shifts, from an analysis of elastic-scattering data, while the other parameter is determined from (15).

The parameters ${}^3r_{LJ}$ for the triplet states cannot be determined from relation (8) alone. In the first analysis for[2] 660 MeV, absorption parameters corresponding to a specific L and averaged over J were introduced. We denote these parameters by $r({}^3P_{0,1,2})$ and $r({}^3F_{2,3})$ for L = 1 and 3, respectively:

$$(r({}^3P_{0,1,2}))^2 = \frac{1}{9}\sum_{J=0}^{2}(2J+1)({}^3r_{1J})^2,$$

$$(r({}^3F_{2,3}))^2 = \frac{1}{12}\sum_{J=2}^{3}(2J+1)({}^3r_{3J})^2.$$

We note that we have $r({}^3F_4) = 1$ and that this parameter was omitted during the averaging. We then find from (8) and (10)

$$\frac{1}{2}\pi\lambda^2[9\{1-(r({}^3P_{0,1,2}))^2\} + 12\{1-(r({}^3F_{2,3}))^2\}] = \sigma(pp\pi^0) + {}^3a\sigma(np\pi^+), \qquad (16)$$

where ${}^3a = \sigma[(np)_P\pi^+]/\sigma(np\pi^+)$ and ${}^1a + {}^3a = 1$. One of the parameters $r({}^3P_{0,1,2})$ and $r({}^3F_{2,3})$ can be determined by analyzing elastic-scattering data, and the other can be determined from Eq. (16). The introduction of these average parameters does not significantly affect the real parts of the phase shifts.[31]

Absorption parameters averaged over L were used in ref. 32; the results agree with those found through the use of $r({}^3P_{0,1,2})$ and $r({}^3F_{2,3})$.

Real parts of the phase shifts. In ordinary phase-shift analysis the scattering is described by means of a finite number of phase shifts, which are determined in the course of the analysis; the other phase shifts are set equal to zero. This procedure is usually improved through explicit inclusion of one-pion exchange in all states having the higher angular momentum.[16] The physics on which this approach is based was described in Secs. 1 and 2: The long-range nuclear forces are due primarily to one-pion exchange.[14,15] The scattering amplitude is written in the form

$$M = M(\delta, r) + M_{\text{OPEC}}(L > L_I), \qquad (17)$$

where $M(\delta, r)$ is the contribution of a limited number of real parts of phase shifts δ and absorption parameters r for $L \leq L_I$; $M_{\text{OPEC}}(L > L_I)$ is the contribution of one-pion exchange to the states with $L > L_I$. The L_I value corresponds to the boundary between the outer and intermediate force ranges and can be found approximately from the relation $L_I + 1/2 \approx 1.5\hbar k/\mu_\pi c$.

In our analysis scheme the real parts of the phase shifts δ can be varied around the values found from extrapolation of solution 1 for lower energies. This restriction may help us avoid the false solutions which arise because of the scarcity of experimental data. The analysis method was further developed in ref. 5. The new scheme contains explicitly the contributions from one-boson exchange in states having intermediate angular momentum values. Expression (17) for the scattering amplitude is replaced by

$$M = M(\delta, r) + M_{\text{OBEC}}(L_{II} < L \leqslant L_I) + M_{\text{OPEC}}(L > L_I), \quad (18)$$

where $M(\delta, r)$ is the contribution from δ and r for $L \leq L_{II}$, $M_{\text{OBEC}}(L_{II} < L \leq L_I)$ is the contribution of one-boson exchange in states with $L_{II} < L \le L_I$, and MOPEC ($L > L_I$) is the same as in Eq. (17). The quantity L_{II} corresponds to the boundary between the core and the intermediate force range and is evaluated from the relation $L_{II} + 1/2 \approx 0.5\hbar k/\mu_\pi c$.

This scheme significantly reduces the number of parameters and consequently it is extremely useful at higher energies – above, say, 1 GeV – in which more partial waves participate in the scattering. This question is discussed in detail in Sec. 5.

Validity of the resonance model for pion production. Mandelstam showed that the resonance (3,3) model qualitatively explains most experiments on pion production in p–p collisions between 400 and[3] 660 MeV. It follows from this model that there should be no appreciable pion production by necleons in states having a total isotopic spin T = 0. The measured pion-production cross section in these states can be used as a good test of the model. This cross section, σ_0, is given, in accordance with charge independence, by the relation

$$\sigma_0 = 3\{2\sigma(np \to \pi^-) - \sigma(pp \to \pi^0)\}, \tag{19}$$

where the factor 3 arises because of the variety of charge states of the pions emitted in n–p collisions. The experimental results, written as the ratio σ_0/σ_1, where σ_1 is the pion-production cross section for p–p collisions (T = 1), are $\sigma_0/\sigma_1 = 0.41 \pm 0.25$ for[33] 590 MeV and $\sigma_0/\sigma_1 \approx 0.2$ for[34] 970 MeV.

These results show that absorption predominates in T = 1 states.

The resonance model can also be checked by a more direct method, by determining the ratio of probabilities for transitions to states having isospins $I_{\pi N} = 1/2$ and $I_{\pi N} = 3/2$. These probabilities have been measured for[35] 650 MeV. The cross sections for the reactions

$$p + p \to p + n + \pi^+; \tag{20}$$

$$p + p \to p + p + \pi^0 \tag{21}$$

are expressed in terms of the two isospin amplitudes A_1 and A_3 under the assumption that the pion and one of the nucleons form a subsystem in the final state; here the indices denote $2I_{\pi N}$. Alternatively, the cross sections are expressed in terms of the amplitudes B_0 and B_1 under the assumption that the emitted nucleons make up the subsystem; in this case the indices represent the nucleon isospin. To experimentally determine amplitudes A_1 and A_3 and the phase difference between these amplitudes we must measure three independent quantities. Two of them are the cross sections for reactions (20) and (21). The third quantity is the spatial asymmetry with respect to neutron and proton exchange in reaction (20);[36] this asymmetry results from the interference between T = 1 and T = 0 states of the emitted nucleons.

We can thus find $|B_0|^2$, $|B_1|^2$, and the term corresponding to interference between B_0 and B_1; equivalently, we can find $|A_1|^2$, $|A_3|^2$, and their phase difference. The probability for a transition to the $I_{\pi N} = 3/2$ state which is found in this manner is 72 ± 3% at[35] 650 MeV, in support of the approximate validity of the resonance model.

The resonance pion-production model used in our analysis scheme is a generalization of the original Mandelstam mode. Absorption in the $^3F_{2,3}$ states [Eq. (10)] and production in the D state [Eq. (11)] have been taken into account because of the following considerations: 1) Analysis of data on elastic p–p scattering at 660 MeV showed that absorption in $^3F_{2,3}$ states cannot be neglected.[2,31] According to a repeated analysis of the data on inelastic p–p scattering at[37] 660 MeV, inclusion of transitions from $^3F_{2,3}$ states significantly improves the agreement with inelastic data also. 2) The angular distribution of neutrons produced in the reaction $pp \to np\pi^+$ at 970 MeV can be approximated by the polynomial[38] $1 - 1.63\cos^2\theta + 7.66\cos^4\theta$, whose last term explicitly shows the importance of production in the D state at this energy.

4. PHASE SHIFTS OF NUCLEON–NUCLEON SCATTERING BETWEEN 400 MeV and 1 GeV

Phase shifts for p – p scattering at 660 MeV. An extensive series of experiments on p–p scattering near 660 MeV was carried out[6)] at Dubna.[39–45] The method described in Sec. 3 was first used to analyze data on the differential cross section, polarization, and depolarization.[2] The set of phase shifts determined in this manner was found to be in satisfactory agreement with the triple-scattering parameters C_{kp}, C_{nn}, and R (later measured in refs. 4 and 44) and in qualitative agreement with other values of the parameter[45] A.

In the analysis described in ref. 2, the phase shifts for the higher-order waves (L > 5) were less than 4° and were set equal to zero. The analysis can obviously be improved by using for these states the values found from the model of one-pion exchange. Further improvements can be made by analyzing the absorption parameters more rigorously than in the first analysis. Improved analyses of all these results have been carried out at Dubna,[31,46–50a] Kyoto,[32] and[51] Livermore.[7)] There have been some differences in the analysis of absorption parameters. Azhgirei et al.[31] used the method of ref. 2 and the absorption parameters for fixed L averaged over J, and then carried out a variation without averaging over J.[47–49] Hama and Hoshizaki[32] reported an analysis based on the absorption parameters for a given J, but averaged over L. MacGregor et al.[51] used as initial absorption parameters the values calculated by Amaldi et al.[10] on the basis of the one-pion-exchange model for pion production.

Despite the variety of approaches which have been used, the real parts of the phase shifts obtained by the various groups have been in surprisingly satisfactory agreement, especially for the lower-order partial waves. The false solution found previously in the purely kinematic analysis[46] dropped out after measurement of the parameter[47] A. As was reported recently,[50] the "new" solution does not seem particularly new; it belongs to the group of solutions mentioned above, as can be seen by comparing the scatter in the data for the solutions obtained by the various groups. The real parts of the phase shifts for the lower-order partial waves for p–p scattering at 660 MeV have thus been unambiguously established, at least qualitatively.[8)] These real parts are shown

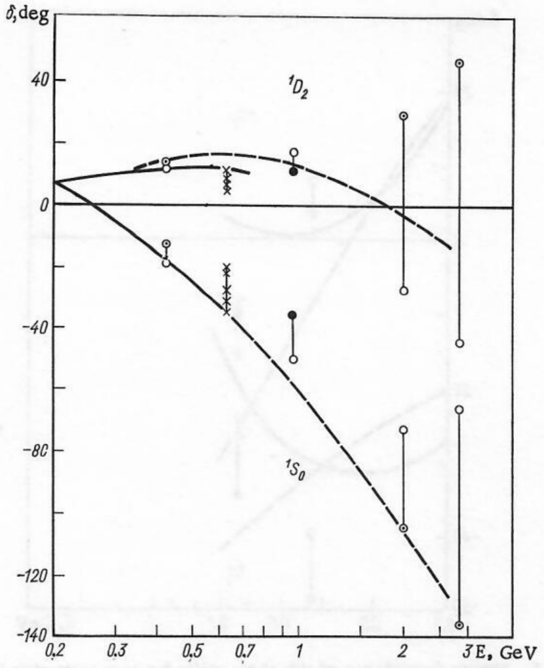

Fig. 1. Energy dependence of the phase shifts for p–p scattering. The phase shifts are taken from the following solutions: JKL-1,[55] MAW-2[51] (400-430 MeV); HH,[32] A-4,[49] KLPYa-1,[61] K-Sh,[50] MAW-2, MAW-4[51] (630-660 MeV); HK-a, HK-b[59a] (970 MeV); H-a, H-á[9] (2 GeV); H-A, H-A'[9] (2.85 GeV). The vertical lines show the scatter in the solutions for each energy. The solid curves below 750 MeV show solution 4 of the energy-dependent analysis carried out at Livermore.[51] For comparison we have also shown the values predicted by the potential model with a hard core (dashed curves).[19,76]

in Figs. 1–4 and Table 3 in Appendix 2. The solution obviously corresponds to solution 1, found below 400 MeV.

There is still much uncertainty regarding the absorption parameters; the values found by various groups have not always been consistent. Nevertheless, there are certain general features: 1) the peripheral nature of the absorption and 2) the pronounced absorption in the F state.

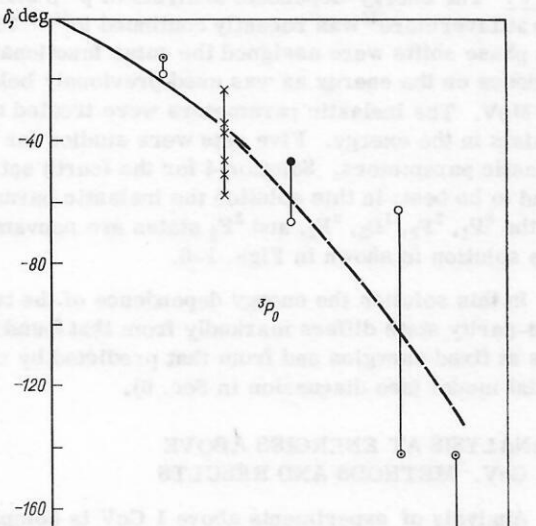

Fig. 2. Energy dependence of the phase shifts for p–p scattering. The notation and references are the same as in Fig. 1.

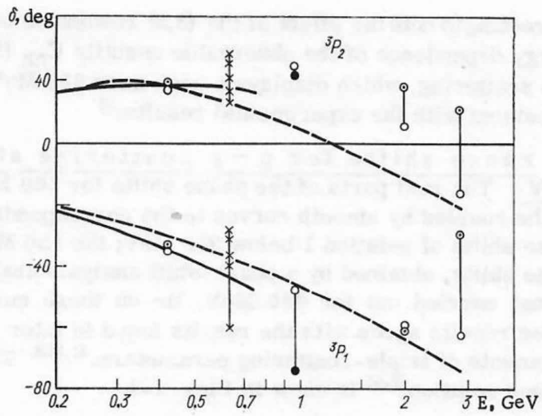

Fig. 3. Energy dependence of the phase shifts for p–p scattering. The notation and references are the same as for Fig. 1.

These features can be seen from Fig. 8, which shows the absorption parameters for fixed L and averaged over J as functions of the impact parameter b, defined as b = (L + 1/2)ƛ.

Observation of feature 2) improved the initial Mandelstam model. Vovchenko derived a model which also describes pion production from F states; his calculations led to an overdetermination of the model parameters, and he calculated the absorption parameters without using elastic-scattering data.[37] The results confirm general feature 1), but certain details differ from the results of the phase-shift analyses cited. Considerable absorption was found in the $^3P_1$ state, and relatively little was found in the $^3F_3$ state. On the other hand, this type of absorption is predicted by one of the Livermore solutions.[51] Accordingly, the discrepancies in the absorption parameters apparently should not affect the uncertainty regarding the real parts of the phase shifts, although a phase-shift analysis based on the results of ref. 37 would be desirable.[9)]

The peripheral nature of the absorption results primarily from the presence of the (3,3) resonance. It is

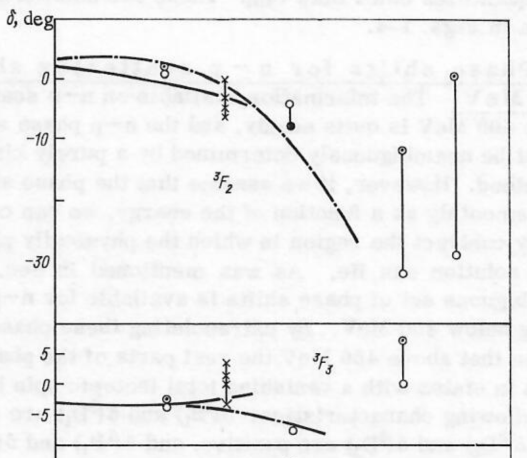

Fig. 4. Energy dependence of the phase shifts for p–p scattering. The dot–dash curves show the results calculated on the basis of the OBEC model;[29] otherwise the notation and references are the same as for Fig. 1.

interesting to note the effect of the (3,3) resonance on the energy dependence of the observable quantity C_{nn} (90°) in p−p scattering, which displays a peak near 600 MeV, in agreement with the experimental results.[52]

<u>Phase shifts for p − p scattering at 430 MeV.</u> The real parts of the phase shifts for 660 MeV can be coupled by smooth curves to the corresponding phase shifts of solution 1 below 310 MeV; the 430 MeV phase shifts, obtained by a phase-shift analysis analogous to that carried out for 660 MeV, lie on these curves.[53] These results agree with the results found in later measurements of triple-scattering parameters.[54,54a] The refined solution[51,55] is show in Figs. 1-4.

<u>Phase shifts[10)] for p − p scattering at 970 MeV.</u> Experiments at this energy were carried out at Birmingham[56–58] and more recently at Saclay.[59] The first phase-shift analysis was carried out by Hama and Hoshizaki[5] by the same method use for 660 MeV, except for a single modification: Degeneracy in the D state, (11), was taken into account. Since there are no triple-scattering data available, the analysis was carried out simply to determine whether the real parts of the phase shifts for solution 1 could be obtained and whether the absorption parameters have the peripheral nature like those found at 660 MeV. The absorption parameters corresponding to central absorption were also studied, and two solutions were found: solution A, corresponding to peripheral absorption, and solution B, corresponding to central absorption. These solutions predicted radically different values for the following observable quantities: D(~ 90°), R(~ 110°), C_{kp}(~ 90°), and C_{nn}(60° ~ 70°). The parameter C_{nn} was measured at Saclay,[59] and the results were found to support solution A.

All the available information, including the C_{nn} values refined by the method using restrictions 1"), 2), and 3), has been analyzed in recent years; the results of this analysis are described in the next section. These results do not rule out either solution A or B.[59a] Accordingly, to choose between these solutions, we must measure observable quantities other than C_{nn}. These two solutions[11)] are shown in Figs. 1-4.

<u>Phase shifts for n − p scattering above 400 MeV.</u> The information available on n−p scattering above 400 MeV is quite scanty, and the n−p phase shifts cannot be unambiguously determined by a purely kinematic method. However, if we assume that the phase shifts vary smoothly as a function of the energy, we can considerably contract the region in which the physically plausible solution can lie. As was mentioned in Sec. 2, an unambiguous set of phase shifts is available for n−p scattering below 400 MeV. By extrapolating these phase shifts we see that above 400 MeV the real parts of the phase shifts in states with a vanishing total isotopic spin have the following characteristics: $\delta(^3S_1)$ and $\delta(^3D_1)$ are negative, $\delta(^3D_2)$ and $\delta(^3D_3)$ are positive, and $\delta(^1P_1)$ and $\delta(^1F_3)$ are both negative.

One of the three sets of phase shifts obtained by Kazarinov and Kiselev[60] for 630 MeV (set 1) definitely displays these features. These investigators analyzed the n−p and p−p data under the assumption of charge independence and through the use of the resonance (3,3) model

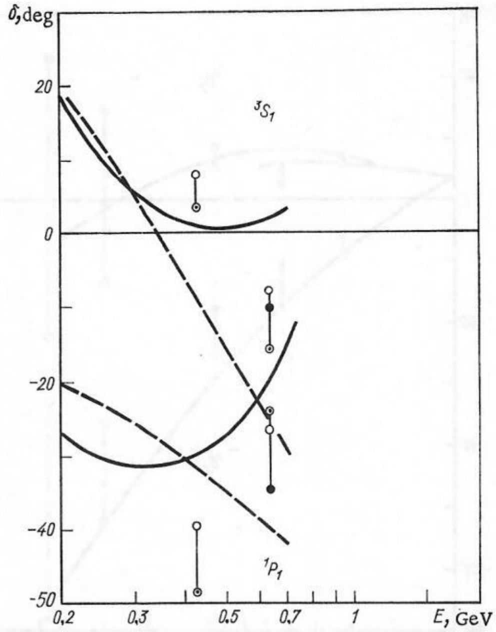

Fig. 5. Energy dependence of the phase shifts for n−p scattering in T = 0 states. The phase shifts are taken from the following solutions: K,[50] MAW-A[62] (400-430 MeV); KLPYa,[61] K-Sh,[50] MAW-A[62] (630 MeV). The solid curves show solution 4 of the energy-dependent analysis carried out at Livermore;[62] the dashed curves were calculated on the basis of a hard-core potential model.[19,76]

for pion production. They used the same p−p data as were used in the p−p analysis for 660 MeV, while they included the differential cross section and the polarization in their data on n−p scattering. The recent measurements of the parameters D and R in elastic n−p scattering at 630 MeV have narrowed the number of possible solutions to two.[61] Solution 1 is retained. The phase shifts of this solution corresponding to the case T = 0 are shown in Figs. 5 and 6.[12)]

<u>Energy-dependent analysis above 400 MeV.</u> The energy-dependent analysis of p−p and n−p data at Livermore[25] was recently continued to[51,62] 750 MeV. The phase shifts were assigned the same functional dependence on the energy as was used previously below[25] 400 MeV. The inelastic parameters were treated as polynomials in the energy. Five sets were studied for the inelastic parameters. Solution 4 for the fourth set was found to be best; in this solution the inelastic parameters for the $^3P_1$, $^3P_2$, $^1D_2$, $^3F_2$, and $^3F_3$ states are nonvanishing. This solution is shown in Figs. 1-6.

In this solution the energy dependence of the triplet even-parity state differs markedly from that found in analyses at fixed energies and from that predicted by the potential model (see discussion in Sec. 6).

5. ANALYSIS AT ENERGIES ABOVE 1 GeV. METHODS AND RESULTS

Analysis of experiments above 1 GeV is complicated by the fact that the information available is completely inadequate for a complete determination of phase shifts. Two assumptions were used in the analysis for 660 MeV: 1) The resonance (3,3) model of Mandelstam was used to

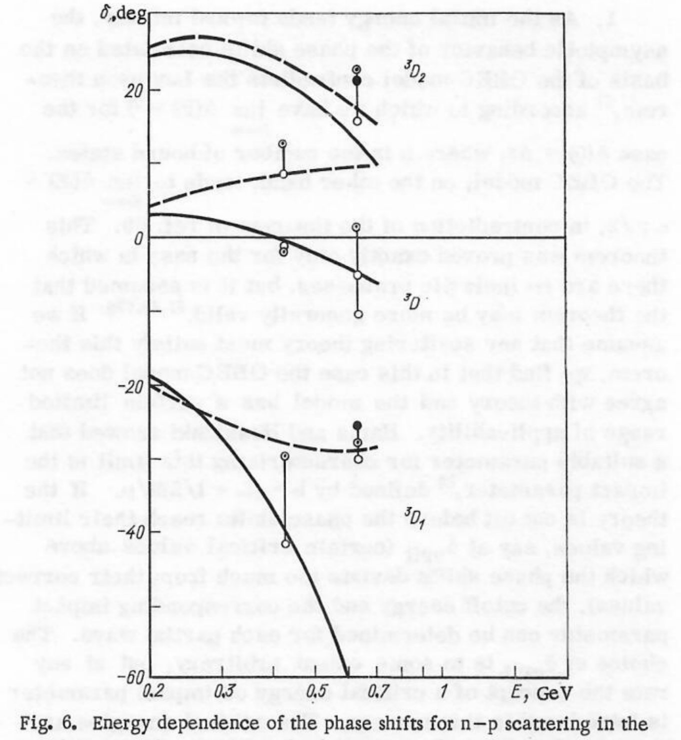

Fig. 6. Energy dependence of the phase shifts for n–p scattering in the T = 0 states. The notation and references are the same as for Fig. 5.

derive the absorption parameters from pion-production data. 2) The real parts of the phase shifts with $L > L_I$ were determined from elastic-scattering data under the assumption that these shifts could be joined smoothly with the values established for lower energies. The phase shifts for $L > L_I$ were taken from the OBEC data. Above 1 GeV, however, assumption 1) is no longer valid. Here a large number of partial waves are involved in the scattering, and the Mandelstam method cannot be used to determine such a large number of absorption parameters. Furthermore, at energies sufficiently above 1 GeV the effect of higher resonances of the πN system cannot be neglected, nor can the production of two or more pions or that of other heavy particles.

Modified account of absorption. In the early approach of Hama and Hoshizaki[7] assumption 1) was replaced by the following: 1') The absorption coefficients can be written as smooth functions of the orbital angular momentum L or of the impact parameter b, defined by $b = (L + 1/2)\bar{\lambda}$.

The function chosen for the absorption coefficients must be such that these coefficients fall rapidly to zero as L increases, since no reaction can occur unless the two nucleons are sufficiently close together. Furthermore, the function must vary over the interval [0, 1]. The following form was thus chosen for this function:[7]

$$1 - r^2(L) = A\exp\{-[(L - L_0)/\gamma]^2\}, \qquad (22)$$

where r(L) is the absorption parameter for the given L, L_0 is a parameter characterizing the point of maximum absorption, and γ is the absorption half-width. In impact-parameter terms, the quantity $L_0 + \gamma$ roughly gives the radius of the nucleon including its pion cloud, and A is a factor which must be determined from the inelastic-scattering cross section. The parameters in Eq. (22) are functions of the parity, spin, and total angular momentum, but we will neglect these dependences here.

Assumption 1') is not purely phenomenological. A more significant improvement of assumption 1) results from applying the general principle of ref. 14 to absorption processes:[11]

1") Absorption near the edge of the nucleon is described correctly by pion theory.

Here the "edge of the nucleon" means the region of two-pion exchange, since in principle there is no absorption in the region of one-pion exchange: Because of the unitarity of the total S matrix, one-pion exchange for pion production leads to absorption in the region of two-pion exchange.

Amaldi et al. calculated the absorption parameters on the basis of the model of one-pion exchange for pion production, taking account of the form factors of the nucleon and the final (3,3) state.[10] Their results, which refer to large distances, can be used as assumption 1"). Then we can state more specifically:

1") The absorption parameters for $L > L_2$ are given correctly by the Amaldi model for one-pion exchange, where L_2 is such that

$$(L + 1/2)\bar{\lambda} \approx \text{the radius for two-pion exchange.} \qquad (23)$$

Substituting, e.g., $(L_2 + 1/2)\bar{\lambda} \approx 10^{-13}$ cm, we find $L_2 = 3$ for 1 GeV and $L_2 = 4$ for 2 GeV. The exact values can be found from the actual analysis. The absorption parameters for $L \le L_2$ must be varied freely.

Real parts of the phase shifts. In addition to restrictions 1') [or 1")] and 2) we require the following:[7]

3) The real parts of the phase shifts for states with intermediate angular momenta must be correctly reproduced by the one-boson-exchange model. The contribution from one-pion exchange for waves having high angular momenta is incorporated as before. The scattering amplitude is given by Eq. (18).

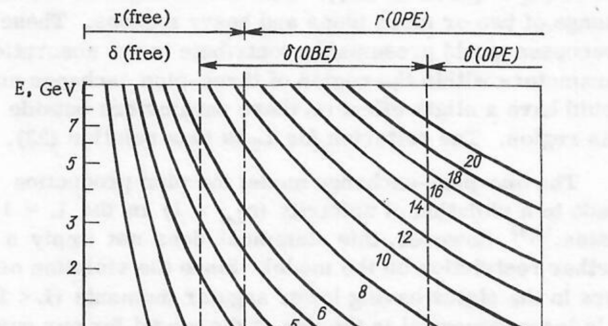

Fig. 7. Relation between the interaction regions and the partial waves. The dependence of the initial kinetic energy in the laboratory system on the impact parameter b is shown for each partial wave. The phase shifts of the waves in each region are treated as shown at the top of this figure.

In the early approaches[7,9] requirement 3) was written as

$$\delta_L = \delta_L(\text{OBEC})\{1 + c(1 - r_L^2)\} \quad (24)$$

for phase shifts having intermediate L. The phase shifts δ_L(OBEC) are calculated from the OBEC model. Parameter c shows the extent to which inelastic processes affect the real parts of the phase shifts.

Using these restrictions, we can significantly reduce the number of free parameters. The situation is illustrated by Fig. 7. At an energy of 2 GeV, e.g., only the phase shifts of states having $L \leq 3$ remain as free parameters.

At present the most reliable method for analyzing data near 1 GeV is apparently that based on the use of assumptions 1"), 2), and 3). The use of this scheme at 970 MeV is described below. Above 2 GeV the Amaldi model in inapplicable (this point is discussed below), so there is no analysis method available other than that based on the use of assumptions 1'), 2), and 3). The results of analyses based on these assumptions carried out for 2 and 3 GeV are discussed at the end of this section.

Applicability limits of the one-pion-exchange model for pion production. The one-pion-exchange model for pion production used above is restricted to certain energy and angular-momentum limits by virtue of the nature of this model.

Meson production between 800 MeV and 1.5 GeV can be described adequately by the model of refs. 62 and 63, but below 800 MeV it does not agree satisfactorily with experimental data, probably because the nucleon–nucleon interaction in the final state is neglected.[13)] Above 1.5 GeV the production of two pions and higher pion–nucleon resonances becomes important, and the model is again inapplicable. The energy limits on the applicability of the model are[64] thus $800\text{ MeV} \lessdot E \lessdot 1.5\text{ GeV}$.

The angular-momentum restriction was mentioned above. The absorption parameters for $L > L_2$ can be predicted correctly by the model, while those for $L \leq L_2$ cannot be [L_2 is given by (23)]. This model neglects the exchange of two or more pions and heavy mesons. These processes would presumably contribute to the absorption parameters within the region of three-pion exchange and would have a slight effect on these parameters outside this region. The criterion for L_2 is thus relation (23).

The one-pion-exchange model for pion production leads to a violation of unitarity ($r_{LJ} > 1$) in the $L = 1$ states.[10,65] However, this statement does not imply a further restriction on the model. Since the violation occurs in the states having lower angular momenta ($L < L_2$), it is inconsequential in the use of the model for our purposes.

Applicability limits of the one-boson-exchange model. In the method described above the use of the OBEC model was restricted to states having intermediate angular momenta, and it was not used in states having lower L. The reasons can be outlined as follows:[66]

1. As the initial energy tends toward infinity, the asymptotic behavior of the phase shifts calculated on the basis of the OBEC model contradicts the Levinson theorem,[67] according to which we have $\lim_{E\to\infty} \delta(E) = 0$ for the case $\delta(0) = n\pi$, where n is the number of bound states. The OBEC model, on the other hand, leads to $\lim_{E\to\infty} \delta(E) = \pm\pi/2$, in contradiction of the theorem of ref. 68. This theorem was proved exactly only for the case in which there are no inelastic processes, but it is assumed that the theorem may be more generally valid.[67,69,69a] If we assume that any scattering theory must satisfy this theorem, we find that in this case the OBEC model does not agree with theory and the model has a certain limited range of applicability. Hama and Hoshizaki showed that a suitable parameter for characterizing this limit is the impact parameter,[68] defined by $b = (L + 1/2)\hbar/p$. If the theory is cut off before the phase shifts reach their limiting values, say at δ_{crit} (certain critical values above which the phase shifts deviate too much from their correct values), the cutoff energy and the corresponding impact parameter can be determined for each partial wave. The choice of δ_{crit} is to some extent arbitrary, but at any rate the concept of a critical energy or impact parameter is introduced in this manner. The critical energies are different partial waves, but the impact parameters have roughly the same critical values. Setting $\delta_{crit} \sim 50°$, we find

$$b_{crit} = 0.4 \sim 0.6\hbar/\mu_\pi c, \quad (25)$$

a value approximately equal to that at the boundary between the intermediate region and the interior core.[68] This result can be interpreted in terms of the internucleon distance r in the following manner: The OBEC model for nuclear forces holds for r larger than b_{crit}. This model must be cut off for $r \lessdot b_{crit}$.

2. Another method for evaluating b_{crit} is in terms of the effective range of the forces due to exchange of intermediate bosons. In the OBEC model it is assumed that the $\pi\pi$ interaction is quite strong, since when nucleons exchange two or more pions, the process is nearly always a separate exchange of heavy mesons (resonance states). Accordingly, each time we introduce a new heavy meson we in principle find a new critical internucleon distance r_{crit}, below which the theory must be corrected for the exchange of as yet unknown heavier mesons. In the OBEC model[29] the heaviest meson is the ω meson, whose mass is assumed equal to $\mu_\omega = 750$ MeV. In this case we have

$$r_{crit} \sim \hbar/\mu_\omega c \sim 0.2\hbar/\mu_\pi c. \quad (26)$$

Actually, there may be some "overfilling," as in the case of pion-exchange forces, leading to an increase in r_{crit}. In the case of pion-exchange forces it was first assumed that the boundary between the OPE region and the intermediate region was at an internucleon distance of about $1\hbar/\mu_\pi c$. According to the TMO potential, however, two-pion exchange forces display an appreciable "overfilling," and the boundary is not at $1\hbar/\mu_\pi c$ but at[70] $\sim 1.5\hbar/\mu_\pi c$. Accordingly, instead of (26) we can choose

$$r_{\mathrm{crit}} \sim 2\hbar/\mu_\omega c \sim 0.4\hbar/\mu_\pi c. \qquad (27)$$

This value agrees with (25).

3. The Yukawa interaction, used in calculations on the basis of the OBEC model, can be treated as a model Hamiltonian whose applicability is governed by a more fundamental interaction. This fundamental interaction predominates in the core region, where the structure of the mesons and the pure nucleons becomes important. In the core region, the Yukawa interaction in the form used in the OBEC model may become meaningless.

Phase shifts for p−p scattering at 970 MeV.[71, 59a] The analysis of p−p scattering for 970 MeV was repeated with new data on C_{nn} and P obtained at Saclay[59] and data on the differential cross section obtained at Birmingham.[56,57] The goal of this analysis was to check the validity of the analysis method based on assumptions 1")-3) and to determine whether to discard solution B found previously on the basis of new data on C_{nn}, which constitute evidence supporting solution A. The real parts of the phase shifts for waves with $L \geq {}^3F_3$ were determined by means of the values found from the one-boson-exchange model.[29] The absorption parameters for $L \geq {}^3F_3$ were taken from the Amaldi OPE model.[65]

This repeated analysis still does not rule out solution A (peripheral absorption) or solution B (central absorption). Further experiments are required to determine which of the solutions is physically correct. The best experiments for this purpose would involve measurement of the depolarization parameter $D(70 \sim 110°)$. Measurements of parameters $A(\theta \geqslant 100)$, $C_{kp}(60\text{–}70°)$, and $A_{xx}(60\text{–}70°)$ could also help in a choice between the two solutions. The following values have been predicted for observable quantities:[59a] for solution A, $D(90°) = 0.71$, $A(120°) = 0.21$, $C_{kp}(70°) = -0.037$, and $A_{xx}(70°) = -0.094$; for solution B, −0.31, −0.19, 0.39, and −0.51, respectively.

Analysis has confirmed the validity of the scheme based on assumptions 1")-3), as can be seen from the values found for χ^2 and from a comparison with the phase shifts found with the values found below 660 MeV. Solutions A and B are shown in Figs. 1-4 and 8 as well as in Table 6 of Appendix 2.

The analysis scheme based on assumptions 1')-3) was also checked at 970 MeV. This scheme was used to analyze data on p−p scattering obtained at Birmingham, and the results of this analysis were compared with earlier results.[7] The parameter values introduced in (22) are

$$\left.\begin{array}{ll} L_0 = 2.1, & \gamma = 1.1 \text{ for solution A;} \\ L_0 = 0.4, & \gamma = 2.5 \text{ for solution B;} \end{array}\right\} \qquad (28)$$

these values should be compared with the corresponding values for 2 and 3 GeV, discussed below.

Phase shifts for p−p scattering at 2 and 3 GeV. Data on the differential cross sections[71,72] and polarization[73] in p−p scattering are available at 2 GeV. These data were analyzed by Hama[9] by a method based on assumptions 1'), 2), and 3). Three solutions were found, two corresponding to solution A at 970 MeV and the third corresponding to solution B. Below we denote these solutions as a, a', and b, respectively.

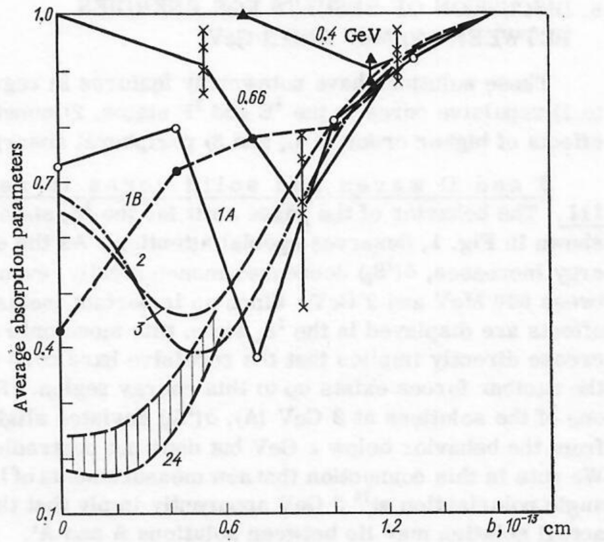

Fig. 8. Dependence of the average absorption parameters on the impact parameter b. The values of $r({}^3F_{2,3,4})$ are shown for the ${}^3F$ states. The results for 24 GeV are shown[13a] only for comparison. Otherwise the references are the same as for Fig. 1.

The parameters governing the absorption take on the values

$$\left.\begin{array}{ll} L_0 = 2.0 \sim 2.2, & \gamma = 2.8 \text{ for solutions } a \text{ and } a'; \\ L_0 = 0.5, & \gamma = 3.8 \text{ for solution } b, \end{array}\right\} \qquad (29)$$

showing that solutions a and a' are solutions for peripheral absorption, while solution b is the solution for central absorption. Solutions a and a' differ in that $\delta({}^1D_2)$ is negative for solution a and positive for a'. The real parts of the phase shifts of the triplet P states for solution b are all negative, while the solutions a and a' have $\delta({}^3P_0)$, $\delta({}^3P_1) < 0$ and $\delta({}^3P_2) > 0$. The real part of the phase shift for the ${}^1S_0$ state is essentially the same for all three solutions.

Measurements of large-angle polarization were reported in ref. 74. These results partially supplement the previous small-angle results used in the analysis. For the new results solution a or a' is apparently to be preferred over solution b. Solutions a and a' are shown in Figs. 1-4.

A similar analysis was carried out by Hama[9] for data on p−p scattering at 3 GeV;[75] three solutions were found with peripheral absorption. The parameters L_0 and γ for these solutions are

$$L_0 = 2.2 \sim 2.5, \quad \gamma = 3.1 \sim 3.7. \qquad (30)$$

These solutions (A, A', and A") differ in the signs of $\delta({}^1D_2)$ and $\delta({}^3P_2)$. For solution A, $\delta({}^1D_2)$ is negative, while for solutions A' and A" it is positive; $\delta({}^3P_2)$ is negative for A and A" but positive for A'.

A choice can be made among the three solutions on the basis of the large-angle polarization data, not available during the analysis. These results[74] constitute evidence against solution A". Solutions A and A' are shown in Figs. 1-4.

6. DISCUSSION OF RESULTS FOR ENERGIES BETWEEN 400 MeV AND 3 GeV

These solutions have noteworthy features in regard to 1) repulsive cores in the ^1E and ^3E states, 2) nonstatic effects of higher order in L, and 3) peripheral absorption.

S and D waves and solid cores in region III. The behavior of the phase shift for the $^1S_0$ state, shown in Fig. 1, deserves special attention. As the energy increases, $\delta(^1S_0)$ decreases monotonically, even between 660 MeV and 2 GeV. Since no important inelastic effects are displayed in the $^1S_0$ state, this monotonic decrease directly implies that the repulsive hard core of the nuclear forces exists up to this energy region. For one of the solutions at 3 GeV (A), $\delta(^1S_0)$ deviates slightly from the behavior below 2 GeV but does not contradict it. We note in this connection that new measurements of large-angle polarization at[74] 3 GeV apparently imply that the actual solution may lie between solutions A and A'.

The $^1D_2$ state is greatly influenced by inelastic effects, so that information about the actual potentials cannot be directly obtained from the real part of the phase shift of this state. However, we can see from Fig. 1 that $\delta(^1D_2)$ for solution *a* at 2 or 3 GeV supports the idea of a hard core in region III. Solution *a'* apparently does not fit this behavior. A choice can be made between these two solutions on the basis of the measurements of C_{nn} and C_{kp} at[9] 1.5-3 GeV.

Potential (1), containing a hard core having a radius of $r_c \approx 0.35\hbar/\mu_\pi c$, can reproduce the experimental phase shifts above 400 MeV quite well, leading to the values[76]

$$\left.\begin{aligned}\delta(^1S_0) &\sim -38°; & \delta(^1D_2) &\sim 10° \text{ for } 660\text{ MeV};\\ &\sim -60°; & &\sim 5° \text{ for } 1\text{ GeV};\\ &\sim -80°; & &\sim -5° \text{ for } 1.5\text{ GeV}.\end{aligned}\right\} \quad (31)$$

The phase shifts shown in Fig. 1 agree quite well with these predictions, supporting the conclusion reached above – that the hard core exists up to an energy on the order of several GeV.

A more quantitative analysis would be of little use at this stage in the development of experiment and theory, but we wish to point out the following circumstance: The $\delta(^1S_0)$ values for 660 and 970 MeV, although they have not been determined very accurately, are slightly above the values predicted by the potential model with a hard core, so it may be appropriate to modify the nonrelativistic picture of completely hard repulsive cores. An upper limit on the "hardness" of the repulsive cores can probably be established. When relativistic effects are neglected, a potential with a soft core having a height on the order of at least 2 GeV can reproduce the $\delta(^1S_0)$ values up to[77] 1 GeV. According to experience gained in calculations in momentum space, however, relativistic effects also lead to a reduction of the magnitudes of the phase shifts,[78] so further experiments and analyses are required in order to reach more definite conclusions.

The phase shift $\delta(^3S_1)$ decreases monotonically from 180° at zero energy to about 0° at 300 MeV. The gradient of this decrease is nearly equal to the gradient of the $\delta(^1S_0)$ decrease. Furthermore, the latest phase-shift analyses of n–p scattering at 630 MeV yield $\delta(^3S_1) = -8.0 \pm 7.7°$, $-13.9 \pm 3.7°$, and $-9.93 \pm 6.99°$ for solutions A and B found at Livermore[62] and for set 1 found[50] at Dubna.[14)] The phase shifts for the T = 0 states are treated as completely elastic, while those for the T = 1 states are fixed by their values found from the analysis of p–p scattering. If we assume that all these values are correct, since they have little effect on $\delta(^3S_1)$, and if we assume that set 2 obtained at Dubna can be discarded (as mentioned in Sec. 4), we conclude that these negative values can be thought of as evidence for a repulsive core in the $^3S_1$ state, which has long been used in various potential models. We note in this connection that the recommended solution of the energy-dependent analysis carried out at Livermore (solution 4) demonstrates the opposite high-energy behavior.[62] Here $\delta(^3S_1)$ is positive and displays a tendency to decrease with increasing energy. This result may mean that the form of the energy dependence selected for this phase shift is still unsatisfactory.

P and F waves and nonstatic effects of higher order in L. Another important consequence of the results of phase-shift analyses for energies above 400 MeV is that there are nonstatic effects of higher order in L in the triplet odd-parity state. Their existence in the singlet even-parity state was established long ago[26] in analysis of energies below 400 MeV.

The results of phase-shift analyses for 660 MeV concerning the triplet odd-parity states can be summarized as follows:

1) The real parts of the phase shifts of the ^3P states split in the manner characteristic of LS potentials.

2) All the real parts of the phase shifts for the ^3F states are small ($\lesssim 6°$).

The first result follows from the interval rule. The interval parameter for the P waves is defined by

$$\rho_P = \{\delta(^3P_0) - \delta(^3P_1)\}/\{\delta(^3P_1) - \delta(^3P_2)\} \quad (32)$$

and is independent of all spin-dependent interactions in the ^3P states. The interval rule takes the same form as in the Born approximation:

$$\left.\begin{aligned}\rho_P &= 0.5 \text{ for LS potentials},\\ \rho_P &= -2.5 \text{ for tensor potentials}.\end{aligned}\right\} \quad (33)$$

The solutions for the phase shifts[49–51,61a] yield

$$\rho_P = (0.1 \text{ to } -0.1) \pm 0.4 \text{ for } 660\text{ MeV}, \quad (34)$$

indicating that the LS potentials apparently predominate in the ^3P states.[15)] The phase shifts for the P states at 660 MeV can be reproduced by the modern potential model having central, tensor, and LS parts.[19] However, this model predicts too large a value for $\delta(^3F_4)$ at 660 MeV ($\gtrsim 15°$) and does not agree even qualitatively with result 2). Accordingly, the effect of the LS interaction in the F states, which does not involve the P states, must be reduced. Nonstatic interactions of higher order in L would naturally lead to such a decrease. By introducing appropriate nonstatic potentials of second order in L, Tamagaki et al.[76,79] were also able to reproduce these phase parameter γ has a weak ($\gamma \propto \ln E$) dependence on the initial energy, so the forward peak contracts as $E \to \infty$, where E is the relativistic energy of the proton in the c.m. system.

Because of the rapid decay of the differential cross sections with increasing θ, we would expect the phase shifts to be governed primarily by the diffraction peak [Eq. (36)]. Higuchi and Machida suggested the following relations:

$$\left.\begin{array}{l} f(\theta)/f(0) \text{ is real,} \\ \text{and} \quad \operatorname{Re} f(\theta)/\operatorname{Im} f(\theta) = \operatorname{Re} f(0)/\operatorname{Im} f(0), \end{array}\right\} \tag{37}$$

where f, the scattering amplitude, is expressed in terms of observables,

$$\left.\begin{array}{l} \operatorname{Re} f(\theta) = \xi \operatorname{Im} f(\theta); \\ \operatorname{Im} f(\theta) = (k\sigma_t/4\pi) \exp(\gamma t/2). \end{array}\right\} \tag{38}$$

Here we have used the optical theorem $\operatorname{Im} f(0) = k\sigma_t/4\pi$, where σ_t is the total cross section and $\xi = \operatorname{Re} f(0)/\operatorname{Im} f(0)$. All the real phase shifts δ_L and absorption parameters r_L are found from relations (38). The results can be summarized as follows:

1) All the δ_L are negative, since all the experimental values of $\operatorname{Re} f(0)$ are negative.

2) The δ_L values tend toward 0 as $E \to \infty$; more precisely, we have $\delta_L \propto (\ln E)^{-1}$, due essentially to the contraction of the forward peak.

3) The absorption parameters indicate peripheral absorption. Their values, which correspond to the longest-range forces, agree with the values of the corresponding absorption parameters for energies below 3 GeV.

In their analysis, Hama and Kawaguchi used as experimental data the differential cross section parametrized in the following form, suitable for all type of scattering:[84]

$$d\sigma/dt \approx A \exp(\gamma t) + (B/k^2E^2) \exp(-ak \sin\theta). \tag{39}$$

They assumed the first term on the right side of this expression to be due to the imaginary part of the amplitude, and the second term to be due to the real part. This assumption differs radically from that incorporated in (37) and leads to the relations

$$\left.\begin{array}{l} \operatorname{Re} f(\theta) = (B'/E) \exp(-ak \sin\theta/2); \\ \operatorname{Im} f(\theta) = (k\sigma_t/4\pi) \exp(\gamma t/2). \end{array}\right\} \tag{40}$$

The use of these expressions led to two phase-shift solutions, both of which yield results different from result 2).

2') Set 1 shows that the δ_L values tend toward 0 according to the law $\delta_L \propto (kE)^{-1}$ as $E \to \infty$.

2") Set 2 shows that the δ_L values tend toward $-\pi/2$ according to the law $\delta_L + \pi/2 \propto (kE)^{-1}$ as $E \to \infty$.

3") The absorption parameters are related most closely to peripheral absorption.

Although at present we cannot check these conclusions, the results are quite interesting, especially in comparison with results for lower energies. The results are shown in Figs. 9 and 10. We see that the real parts of the phase shifts for all these solutions have an energy dependence markedly different from that of phase shifts for lower energies. Guesses can be based on these results, and a variety of models for the interior region itself can be discussed. This discussion, however, lies outside the scope of this paper (see, e.g., refs. 85 and 86).

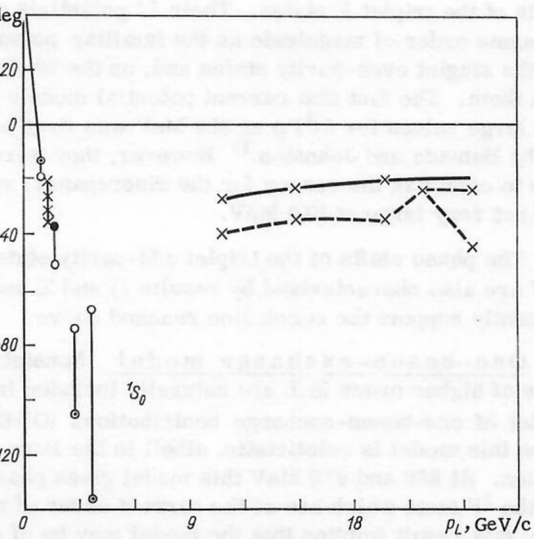

Fig. 9. Dependence of the real parts of the phase shifts on the initial momentum p_L. Shown here are solutions[13] HM-11 (solid curve) and[13a] HK (dashed curves). The results of the analyses for energies below 3 GeV are reproduced here for comparison.

Polarization effects in high-energy scattering. If the values characterizing the polarization turn out to be nonvanishing above 10 GeV, these results will prove incorrect. The assumption of a spin-independent interaction has turned out to be incorrect. Furthermore, since the polarization arises as the result of an interference between different amplitudes of different states,

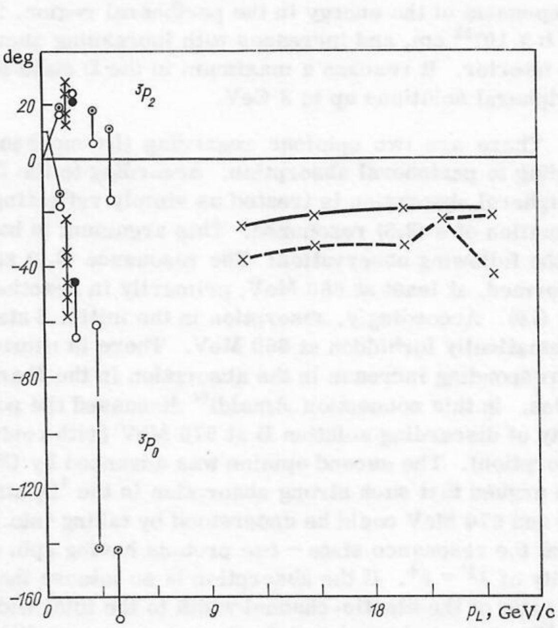

Fig. 10. Dependence of the real parts of the phase shifts on the initial momentum p_L. The literature references are the same as for Fig. 9.

shifts of the triplet F states. Their L^2 potentials are of the same order of magnitude as the familiar potentials for the singlet even-parity states and, on the whole, agree with them. The fact that current potential models predict large values for $\delta(^3F_4)$ at 310 MeV was first pointed out by Hamada and Johnston.[19] However, they were not able to establish the reason for the discrepancy, since it was not very large at 310 MeV.

The phase shifts of the triplet odd-parity states at 1 GeV are also characterized by results 1) and 2) and consequently support the conclusion reached above.

One-boson-exchange model. Nonstatic effects of higher order in L are naturally included in the model of one-boson-exchange contributions (OBEC),[28] since this model is relativistic, albeit in the Born approximation. At 660 and 970 MeV this model gives phase shifts for the ^3F state which are of the correct order of magnitude; this result implies that the model may be of some use above 400 MeV.

The one-boson-exchange model is undoubtedly useful for determining the phase shifts of intermediate and higher-order partial waves above 400 MeV. At present, however, it is not clear whether this model is quantitatively correct. We will cite simply the results of ref. 49, according to which the incorporation of one-boson exchange in the calculation of the phase shifts for states with $J > 6$ significantly improves the description of the new data on small-angle polarization in p–p scattering at[16] 660 MeV.

Peripheral absorption. The inelastic parameters have still not been determined unambiguously, even at 660 MeV, on which energy much attention has been focused. However, all these studies indicate that the absorption is of a peripheral nature. Solutions of this type are available at energies above 660 MeV, as can be seen from Fig. 8, which shows the absorption parameters for fixed L and averaged over J as functions of the impact parameter $b = (L + 1/2)\lambda\!\!\!^{-}$. We see that there is a regularity in the absorption. The absorption intensity is nearly independent of the energy in the peripheral region, i.e., for $b \gtrsim 10^{-13}$ cm, and increases with increasing energy in the interior. It reaches a maximum in the D state for all peripheral solutions up to 3 GeV.

There are two opinions regarding the mechanism leading to peripheral absorption. According to the first, peripheral absorption is treated as simply reflecting the formation of a (3,3) resonance. This argument is based on the following observation: The resonance (3,3) state is formed, at least at 660 MeV, primarily in reactions (9) and (10). Accordingly, absorption in the initial S state is kinematically forbidden at 660 MeV. There is naturally a corresponding increase in the absorption in the D and F states. In this connection Amaldi[64] discussed the possibility of discarding solution B at 970 MeV (with central absorption). The second opinion was advanced by Chew,[80] who argued that such strong absorption in the $^1D_2$ state at 660 and 970 MeV could be understood by taking into account the resonance state – two protons having spin and parity of $J^P = 2^+$. If the absorption is so intense that x, the ratio of the elastic-channel width to the total width in the $^1D_2$ state, is less than 1/2, the resonance condition at energy E_r becomes[80a]

$$(dr(^1D_2)/dE)_{E_r} = 0; \quad (\delta(^1D_2))_{E_r} = 0^\circ. \tag{35}$$

Chew noted that both the available experimental data at 660–970 MeV and the phase shift solutions for them are consistent with this condition. Arndt[12] analyzed this possibility for the two-channel problem. Unfortunately, final conclusions could not be drawn from this analysis, and further study is necessary.

Finally, we give for reference the size of the absorption volume, defined as the square root of the average value of b^2 with a weight factor $(2L + 1)(1 - r_L)$, where r_L is the average absorption parameter. From Fig. 8 we see that this size is $(\langle b^2\rangle)^{1/2} \approx (0.9\text{–}1.1)\cdot 10^{-13}$ cm for all solutions with peripheral absorption. For solution B at 970 MeV we have $(\langle b^2\rangle)^{1/2} \approx 0.6\cdot 10^{-13}$ cm.

7. PHASE SHIFTS IN NUCLEON–NUCLEON SCATTERING ABOVE 10 GeV

Phase-shift analysis above 3 GeV is difficult, since very little experimental information is available. If a phase-shift analysis were carried out at these energies without any theory or model, the result would be a large number of solutions. Higuchi and Machida[13] and Hama and Kawaguchi[13a] analyzed available data on p–p scattering above 10 GeV in an attempt to find the asymptotic behavior of the phase shifts of p–p scattering. A basic assumption in these studies was that the interaction was spin-independent. Recent polarization experiments have shown that the amplitudes for p–p scattering depend on the spins even at an initial energy[81] of about 10 GeV, so this assumption is not valid up to 10 GeV. The phase shifts are still completely unknown for 3–10 GeV.

Above 10 GeV no polarization measurements have been reported yet, and it is unclear to what extent this assumption is valid. Regardless of whether this assumption is valid, the real parts of the phase shifts cannot be neglected even above 10 GeV, as can be seen from the following experimental fact: The real part of the forward-scattering amplitude does not vanish at least up to[82] 30 GeV. In the absence of real parts of the phase shifts, the scattering amplitudes become purely imaginary, so the real parts of the phase shifts do not vanish. Analysis of the angular distributions in the Coulomb-interference region at 10–30 GeV also indicates the importance of the real parts of the phase shifts.[83]

We turn first to the phase shifts obtained in the analyses cited above; then we will discuss the polarization effects, taking up the possibility of finding the real parts of the phase shifts in the case of a spin-dependent interaction.

Phase shift for p–p scattering above 10 GeV. The available experimental information consists of data on total cross sections, angular distributions, and the ratio of the real and imaginary parts of the forward-scattering amplitudes. The angular distribution has a sharp peak in the forward direction, which can be parametrized by the relation

$$d\sigma/dt \approx A\exp(\gamma t); \quad t = -4k^2\sin^2(\theta/2), \tag{36}$$

where $A \approx 40$ mb/(GeV/c)$^{-2}$ and $\gamma \approx 10$ (GeV/c)$^{-2}$. The any assumption neglecting this interference is forbidden. Recent experiments have shown that polarization in p−p scattering is relatively pronounced, even at 10 GeV; its value in the angular range corresponding to forward scattering is about 20% at 4-6 GeV and about 10% at 9-11 GeV. We will briefly discuss which observables are most efficient for obtaining the real parts of the phase shifts.

Polarization effects in high-energy scattering were first analyzed by Lapidus[87] and Hoshizaki and Machida[1] on the basis of the simple disk model. They showed that in the absence of real parts of the phase shifts, some observables vanish. The experimental observation of nonvanishing values may thus imply the existence of nonvanishing real parts of the phase shifts. Let us look at this problem in a more general, relativistic form, without resorting to the disk model. We expand the scattering amplitude in terms of wave functions of the initial spin state:

$$f_i=\sum_j M_{ij}\chi_j, \tag{41}$$

where χ_j is one of the four spin states (there are three triplet states and one singlet state), and M is a function of the scattering angle, a 4 × 4 matrix in spin space. We turn first to the polarization of an initially unpolarized beam scattered by an unpolarized target:

$$P=\langle\sigma_n\rangle_f=\mathrm{Tr}\,(\rho_f\sigma_n)/\mathrm{Tr}\,(\rho_f). \tag{42}$$

Here σ_n is the component of the Pauli matrix normal to the scattering plane, and ρ_f is the 4 × 4 density matrix for the final polarization state, related to the initial density matrix by

$$\rho_f=M\rho_i M^+. \tag{43}$$

For this type of scattering ρ_i is a unit matrix, and $\mathrm{Tr}(MM^+)/4$ is a differential cross section. Denoting this cross section by I_0, we find

$$I_0P=\mathrm{Tr}\,(MM^+\sigma_n)/4, \tag{44}$$

taking the trace, we find

$$I_0P=\left(\frac{\sqrt{2}}{4}\right)\,\mathrm{Im}\,\{(M_{10}-M_{01})^*(M_{11}+M_{00}-M_{1-1})\}, \tag{45}$$

where M_{ij} are the elements of the M matrix in the triplet states. Here the indices 1, 0, −1 refer to the three triplet states, having S_z = 1, 0, −1, respectively. We can conclude from (45) that: 1) If the scattering amplitude is independent of the spin, the elements of the M matrix corresponding to spin flip (M_{10}, M_{01}, M_{1-1}) vanish and the polarization vanishes; 2) if the real parts of the phase shifts vanish, the scattering amplitude and thus M_{ij} become purely imaginary, and the polarization again vanishes. Accordingly, the observation of nonvanishing values of P could be taken as direct evidence for the existence of a spin dependence and the existence of nonvanishing real parts of the phase shifts[88] δ_{LJ}.

As we see from the preceding discussion, observables such as Im A* B, where A and B are linear combinations of M-matrix elements, vanish if the real parts of the phase shifts vanish; these observables are useful tools for extracting information on the real parts of the phase shifts. Other such quantities are the polarization-correlation parameters $C_{n\mu\nu}$, $C'_{n\mu\nu}$, $P_{\alpha\beta n}$, and $P'_{\alpha\beta n}$, which include, e.g., the observables C^n_{kp}, C'^n_{kp}, etc. These parameters were determined in ref. 89. It would be extremely desirable to measure these parameters at a few GeV. Measurements of any triple-scattering parameters would also be useful for studying the spin dependence of the scattering amplitude. If the spin dependence is completely neglected, these parameters become, for n−p scattering,

$$\left.\begin{array}{l} D=1;\ R=\cos(\theta-\theta_L);\ A=-\sin(\theta-\theta_L);\\ R'=-A;\ A'=R;\\ D_t=R_t=A_t=R'_t=A'_t=0;\\ C_{nn}=C_{kp}=C_{kk}=C_{pp}=0;\\ C^n_{kp}=C^n_{pk}=C^n_{pp}=C^n_{kk}=0,\end{array}\right\} \tag{46}$$

where θ and θ_L are the scattering angles in the c.m. and laboratory systems, respectively. For p−p scattering the angular distributions of these parameters are complicated by the Pauli principle, but if there is no spin dependence we find the following relations:

$$\left.\begin{array}{l} R=D\cos(\theta-\theta_L);\ A=-D\sin(\theta-\theta_L);\\ R'=-A;\ A'=R;\\ C_{kp}=-C_{nn}\sin(\alpha+\alpha');\ C_{pp}=C_{kk}=C_{nn}\cos(\alpha+\alpha');\\ C^n_{pk}=-C^n_{kp};\ C^n_{pp}=C^n_{kk}=C^n_{kp}\,\mathrm{tg}\,(\alpha+\alpha'),\end{array}\right\} \tag{47}$$

where $\alpha=\theta/2-\theta_L$, $\alpha'=\theta'/2-\theta'_L$, and θ' and θ'_L are the scattering angles of the recoil particle in the c.m. and laboratory system, respectively. Any deviation of the experimental values from relations (46) or (47) would imply a spin dependence of the scattering amplitude.

APPENDIX 1

DETERMINATION OF THE PHASE SHIFTS IN BOUND STATES

To determine the phase shifts in states which are bound, according to the angular momentum, we write the elastic-scattering matrix as

$$S=\exp(i\delta)\,X\exp(i\delta), \tag{A.1}$$

where δ is a diagonal 2 × 2 matrix with elements $\delta_{LJ}+i\chi_{LJ}$. Introducing the absorption parameter $r_{LJ}=\exp(-2\chi_{LJ})$, we find

$$\exp(i\delta)=\begin{pmatrix} r_-^{1/2}\exp(i\delta_-) & 0\\ 0 & r_+^{1/2}\exp(i\delta_+)\end{pmatrix}, \tag{A.2}$$

where $r_\mp=r_{J\mp1,J}$ and $\delta_\mp=\delta_{J\mp1,J}$. The quantity X is a symmetric 2 × 2 matrix, which describes the mixing of states with L = J − 1 and L = J + 1. Matrix S is a symmetric 2 × 2 matrix, so it represents six real parameters, four of which are $\delta_\mp$ and $r_\mp$. The other two are the mixing parameter and its phase. These parameters can be introduced by writing the off-diagonal elements of matrix X as $i\rho_J\exp(i\varphi_J)$. The diagonal elements of matrix X are determined from the requirement that the unitarity condition have the form

$$S^{+}S=\begin{pmatrix} r_-^2 & r^J \\ r^{J*} & r_+^2 \end{pmatrix}. \quad \text{(A.3)}$$

Here r^J is some function of $r_{\pm}$, ρ_J, and φ_J. Introducing $\rho=\rho_J$ and $\varphi=\varphi_J$, we find from (A.1)-(A.3)

$$X=\begin{pmatrix} (1-(r_+/r_-)\,\rho^2)^{1/2} & i\rho\exp(i\varphi) \\ i\rho\exp(i\varphi) & (1-(r_-/r_+)\,\rho^2)^{1/2} \end{pmatrix}; \quad \text{(A.4)}$$

$$r^J=i\rho\,(r_-r_+)^{1/2}\exp\left[i\,(\delta_--\delta_+)\right]$$
$$\times\{r_+[1-\rho^2\,(r_-/r_+)]^{1/2}\exp(i\varphi)-r_-[1-\rho^2\,(r_+/r_-)]^{1/2}\exp(-i\varphi)\}. \quad \text{(A.5)}$$

Equations (A.1)-(A.4) illustrate the parametrization which we have used in Eq. (5) in the text proper. Physically, relation (A.1) means that two states are mixed in that part of the interaction which corresponds to the core. This parametrization is a generalization of Stapp's parametrization,[18] which is used at energies below the meson-production threshold. In an alternative parametrization, used in the analyses carried out at Livermore,[51] the S matrix is written as

$$S=\begin{pmatrix} \cos\rho_-\cos 2\varepsilon\exp(2i\delta_-) & i\sin 2\varepsilon\exp\left[i\,(\delta_-+\delta_++\alpha)\right] \\ i\sin 2\varepsilon\exp\left[i\,(\delta_-+\delta_++\alpha)\right] & \cos\rho_+\cos 2\varepsilon\exp(2i\delta_+) \end{pmatrix}. \quad \text{(A.6)}$$

In this definition the unitary condition is not as simple as in Eq. (A.3), since the absorption depends not only on $\cos\rho_{\pm}$ but also on the mixing parameter ε. The two definitions are related by

$$\left.\begin{aligned} &\sin 2\varepsilon=\rho\,(r_+r_-)^{1/2};\\ &\cos\rho_+=r_+\{[1-\rho^2\,(r_-/r_+)]/(1-\rho^2r_+r_-)\}^{1/2};\\ &\cos\rho_-=r_-\{[1-\rho^2\,(r_+/r_-)]/(1-\rho^2r_+r_-)\}^{1/2};\\ &\alpha=\varphi;\ \delta_-=\delta_-;\ \delta_+=\delta_+. \end{aligned}\right\} \quad \text{(A.7)}$$

TABLE 1. Phase-Shift Solution (T = 1) at 400-430 MeV

Solution	JKL-1 (ref. 55)	MAW-2 (ref. 51)
χ^2	79.2	92.6
Number of points	$83\,(p-p)+29\,(n-p)$	96
Energy, MeV	400	425
Real parts of the phase shifts, deg		
$^1S_0$	-13.46 ± 1.78	$-19.35\pm2,05$
$^1D_2$	12.81 ± 0.52	$10.91\pm1,36$
$^1G_4$	2.21 ± 0.28	1.42 ± 0.51
$^3P_0$	-13.50 ± 1.91	-18.19 ± 2.68
$^3P_1$	-33.80 ± 0.81	-34.63 ± 1.40
$^3P_2$	18.20 ± 0.50	17.18 ± 1.30
ε_2	-1.11 ± 0.69	-1.43 ± 0.89
$^3F_2$	1.77 ± 0.57	0.87 ± 1.22
$^3F_3$	-2.55 ± 0.43	-3.71 ± 0.63
$^3F_4$	3.68 ± 0.27	3.31 ± 0.72
ε_4	|	-1.86 ± 0.48
$^3H_4$	|	0.08 ± 0.59
$^3H_5$	OPEC	-2.07 ± 0.53
$^3H_6$	↓	0.35 ± 0.35
Absorption parameters*		
$^1D_2$	3.69 ± 0.94	23.46

*Here $r_{LJ}=\exp(-2\chi_{LJ})=\cos\rho_{LJ}$. The value of χ_2 is given in the JKL-1 solution, and the value of ρ_2 is given in the MAW-2 solution.

The inverse relations are

$$\left.\begin{aligned} &r_+=(\cos^2\rho_+\cos^2 2\varepsilon+\sin^2 2\varepsilon)^{1/2};\\ &r_-=(\cos^2\rho_-\cos^2 2\varepsilon+\sin^2 2\varepsilon)^{1/2};\\ &\rho=\sin 2\varepsilon/(r_+r_-)^{1/2};\\ &\varphi=\alpha;\ \delta_-=\delta_-;\ \delta_+=\delta_+. \end{aligned}\right\} \quad \text{(A.8)}$$

In the calculations of Amaldi et al.[10] an absorption matrix ^0R was introduced in correspondence with the elastic-unitarity condition, written as $S^+S=1-{}^0R$, where for bound states we have

$${}^0R=\begin{pmatrix} {}^0R_{J-1,\,J} & {}^0R^J \\ {}^0R^{J*} & {}^0R_{J+1,\,J} \end{pmatrix}. \quad \text{(A.9)}$$

Comparing (A.3) and (A.9), we find

$$\left.\begin{aligned} &{}^0R_{J-1,\,J}=1-r_-^2;\\ &{}^0R_{J+1,\,J}=1-r_+^2;\\ &{}^0R^J=r^J \end{aligned}\right\} \quad \text{(A.10)}$$

where r^J is given by (A.5).

APPENDIX 2

SUMMARY OF SETS OF PHASE SHIFTS ABOVE 400 MeV

The phase-shift solutions available between 400 MeV and 3 GeV are shown in the accompanying tables. The most recent solutions obtained by each group of investigators[17] are given (except for one of the recent solutions found for 660 MeV at Dubna[50a]). Earlier solutions are not shown here, nor are the MAW-1 and MAW-3 solutions for[51] 630 MeV, since these solutions were used as initial sets in the calculation of solutions MAW-2 and MAW-4 (which are shown).

TABLE 2. Phase-Shift Solutions (T = 0) at 400-430 MeV

Solution	JKL-1 (ref. 55)	MAW-2 (ref. 62)
χ^2		22.9
Number of points	—	30
Real parts of phase shifts, deg		
$^1P_1$	-48.43 ± 2.15	-39.44 ± 3.64
$^1F_3$	-3.59 ± 1.30	-6.01 ± 0.55
$^1H_5$	(OPEC)	$(-2.19)_{\mathrm{OPEC}}$
$^3S_1$	3.42 ± 3.68	8.13 ± 2.90
ε_1	4.79 ± 2.97	-4.85 ± 2.61
$^3D_1$	-29.66 ± 2.74	-41.41 ± 2.90
$^3D_2$	12.44 ± 2.96	8.65 ± 3.74
$^3D_3$	-1.79 ± 1.59	-1.31 ± 1.69
ε_3	7.70 ± 0.88	8.98 ± 0.99
$^3G_3$	-0.66 ± 1.77	1.18 ± 1.21
$^3G_4$	3.90 ± 0.88	0.39 ± 3.02
$^3G_5$	-2.81 ± 2.18	-1.45 ± 1.13

TABLE 3. Phase-Shift Solutions* (T = 1) at 630-660 MeV

Solution	HH (ref. [32])	A-4 [49]	VZK-A (ref. 96)	BGKK-III [93]	MAW-2 [51]	MAW-4 [51]
χ^2	31.1	93.4	75	198,5	204,8	195,7
Number of points	45	118	110	191 ($pp+np$)	169	169
Energy, MeV	660	657	640	630	630	630
Real parts of phase shifts, deg						
$^1S_0$	−32	−32.2±12.1	−23.3±3.9	−19.81±3.38	−20.68±9.41	−35.31±4.88
$^1D_2$	10	4.9±6.0	11.2±3.1	9.26±1.58	9.01±7,17	3.73±5.16
$^1G_4$	4.5	5.3±2.5	5,2±1,3	5.52±0,66	3.48±2.45	4.13±2,17
$^3P_0$	−51	−37.6±15.5	−59.0±6.7	−20.69±2.74	−34.34±8,83	−57,51±12.84
$^3P_1$	−37	−31,6±5.8	−35.8±4.5	−29.95±2.19	−40.20±3.80	−61,25±11.43
$^3P_2$	16	25.3±4,2	20.5±2.5	34.82±1,77	27,91±2.71	13,15±3,48
ε_2	−3	−2.1±5.4	−3.7±2.1	3.00±0.89	−1.13±2.65	−2.92±2.49
$^3F_2$	−4	−3,5±2,7	−5,4±2.2	−4,20±0.60	−0.23±3.28	−6.50±2.81
$^3F_3$	3.5	−0.6±7.8	4.6±2.3	0,69±0,77	2.99±1,89	−0,09±2.77
$^3F_4$	3	2,5±1.0	2.3±0.8	3,64±0.81	4.76±1.59	2.91±1,69
ε_4	−5.25	−4.8±1.8	−2.9±1.1	0,76±0.76	−1,50±1.23	−2,59±1.08
$^3H_4$	0.75	−1.2±1.8	1.5±1,3	−2,15±0.60	4,39±0.99	−0.18±1.17
$^3H_5$	−1,25	−2,6±1.3	1.3±0.9	−3.21±0.79	0.18±0,95	2.09±1.47
$^3H_6$	0.75	−0,1±0.8	1,9±0.5	−2.70±0,45	2.32±0,53	0,53±0.17
Absorption parameters**						
$^1S_0$	(1.0)	(1.0)	(0.0)	(0,0)	(0.0)	(0.0)
$^1D_2$	0.64	0.66±0.04	7.3±0,6	10.96±2.56	42.6	37.8
$^1G_4$	(1.0)	(1.0)	(0.0)	(0.0)	(0.0)	28.7
$^3P_0$	0.98	0.79±0.19	0.7±4.9	(0.0)	(0.0)	12,8
$^3P_1$	0,98	1,18±0.37	6.8±4.5	(0.0)	14.1	54.5
$^3P_2$	0.90	0.79±0.24	2,4±2.0	5,37±1,52	34.2	17.0
ε_2	(0.0)	(0,0)	(0,0)	(0.0)	(0.0)	−76.0
$^3F_2$	0.90	0.95±0.10	7.2±2.0	0,57±1.07	38.4	24,0
$^3F_3$	0.68	0.64±0.08	5.6±1.7	2.32±1.52	25.0	13.5
$^3F_4$	(1.0)	(1.0)	(0.0)	4.14±0.73	(0.0)	(0.0)

*The indicated phase-shift errors, calculated from the error matrix, do not always accurately reflect the uncertainty in the phase-shift solutions.[51]

**Here $r_{LJ} = \exp(-2\chi_{LJ}) \cos \rho_{LJ}$. The r_{LJ} values are given in solutions[32] HH and[49] A-4; the χ_{LJ} values are given in the[96] VZK-A and[93] BGKK-III solutions; and in the MAW-2 and MAW-4 solutions[51] the values of ρ_{LJ} are given. For unbound states, these latter values are determined from the relation given above, while for bound states they are determined from Eq. (A.6) of Appendix 1.

TABLE 4. Phase-Shift Solutions* (T = 0) at 630 MeV

Solution	BGKK-III [93]	MAW-A [62]
χ^2	198.5	115.1
Number of points	191 ($pp+np$)	77
Real parts of phase shifts, deg		
$^1P_1$	−27.30±5.39	−26.38±6.95
$^1F_3$	−6.36±2.06	−12,56±1.90
$^1H_5$	6.24±1.44	2,20±1.99
$^3S_1$	−17.40±5.44	−8.03±7.68
ε_1	9.48±5.15	7.81±3.34
$^3D_1$	−27.30±2.41	−29.94±2.83
$^3D_2$	22.53±3.16	15.80±2.57
$^3D_3$	8.87±1.82	1.64±1.15
ε_3	9.79±1.70	14.99±0,83
$^3G_3$	−6.13±2.17	−4.41±2.10
$^3G_4$	6.02±1.36	2.55±2.17
$^3G_5$	−7.02±1.17	−6.87±1.30
ε_5	(OPEC)	8.45±0.79

*See the first note in Table 3.

TABLE 5. Phase-Shift Solutions* of the solution-2 ("False") Type at 630 MeV

Solution	BGKK-II [93]	MAW-B [62]
χ^2	248.3	114.5
Number of points	191 ($pp+np$)	77
$^1P_1$	−39,66±10,49	−18.54±3,43
$^1F_3$	2,19±2,69	6.88±1.86
$^1H_5$	−2.54±0.94	$(-2.53)_{OPEC}$
$^3S_1$	−6,01±7.43	−13,89±3.65
ε_1	20.67±4.91	19.07±1.58
$^3D_1$	32.82±10.11	20.08±3,06
$^3D_2$	21,00±4.36	17.41±2.34
$^3D_3$	0.15±2.77	4.80±1.04
ε_3	8.68±3.14	14.78±1.28
$^3G_3$	1.41±2.15	−3.78±1.34
$^3G_4$	1,10±2.24	10.33±1.23
$^3G_5$	−1,90±1.12	−5.33±0.79
ε_5	(OPEC)	$(5,02)_{OPEC}$

*See the first note in Table 3.

TABLE 6. Phase-Shift Solutions* (T = 1) at 970 MeV

Solution	HK—a	HK—b	HK—a	HK—b
χ^2	51.8	40.7	—	—
Number of points	60	60	—	—
	Real parts of phase shifts, deg		Absorption parameters	
$^1S_0$	−50.8	−36.6	0.727	0.433
$^1D_2$	16.0	10.5	0.379	0.777
$^1G_4$	$(4.50)_{OBE}$	—	$(0.919)_{OPE}$	—
$^1I_6$	$(0,669)_{OBE}$	—	$(0.986)_{OFE}$	—
$^3P_0$	−65.9	−46.5	1.00	0.561
$^3P_1$	−48,6	−75.1	0.807	0.900
$^3P_2$	23.4	21.0	0.744	0.613
ρ_2, $\varphi_2^\dagger$	0.083	0.272	−2.13+	51.4+
$^3F_2$	−4.62	−8.09	0.512	0.467
$^3F_3$	$(-7.73)_{OBE}$	—	$(0,725)_{OPE}$	—
$^3F_4$	$(6.50)_{OBE}$	—	$(0.993)_{OPE}$	—
ρ_4, $\varphi_4^\dagger$	$(-0.079)_{OBE}$	—	(0.0)+	—
$^3H_4$	$(1.10)_{OBE}$	—	$(0.984)_{OPE}$	—
$^3H_5$	$(-2.00)_{OBE}$	—	$(0.955)_{OPE}$	—
$^3H_6$	$(2,40)_{OBE}$	—	$(0.998)_{OPE}$	—

* The mixing parameter ρ_J and its phase φ_J are found from relation (5) in the text proper. The φ_J values are given in degrees.

TABLE 7. Phase-Shift Solutions (T = 1) at 2 and 2.85 GeV

Energy, GeV	2			2.85		
Solution	H − *a*	H − *a*'	H − b	H − A	H − A'	H − A"
χ^2	26.0	25.4	28.2	59.8	53.6	52.9
Number of points	28	28	28	62	62	62
Real parts of phase shifts, deg						
$^1S_0$	−73.3	−105.1	−70.0	−66.8	−136.5	−120.0
$^1D_2$	−27.9	29.2	−19.0	−45.5	44.3	46.0
$^3P_0$	−62.6	−142.1	−54.4	−168.3	−143.2	−176.0
$^3P_1$	−60.8	−61.6	−61.2	−63.4	−30.3	−63.3
$^3P_2$	5.1	16.9	−2.8	−16.4	10.1	−15.9
ε_2	16.9	23.4	25.2	19.0	30.1	20.0
$^3F_2$	−31.7	−12.0	−63.6	−28.8	0.5	−25.6
$^3F_3$	0.0	7.3	−0.5	−6.7	−12.8	−8.0
$^3F_4$	−2.3	4.7	0.0	5.7	4.1	4.3
Absorption parameters*						
L_0	1.97	2.24	0.52	2.20	2.54	2.27
γ	2.83	2.79	3.79	3.71	3.10	3.53
c	1.54	1.32	−0.01	0.58	−0.03	0.31

*Absorption parameters r(L) can be calculated from L_0 and γ on the basis of relation (22). The values of parameter A in Eq. (22), found from the cross section for inelastic scattering, are 0.854, 0.794, 0.989, 0.793, 0.883, and 0.827 for solutions *a*, *a*', and b at 2 GeV, and A, A', and A" at 2.85 GeV, respectively.

*Publisher's note: During translation of the original article [reprinted from Progress of Theoretical Physics, Supplement No. 42 (1968)] into Russian, references 90-108 were added by the Russian editor to update the material.

1)The results of a recent analysis of p−p and n−p data at energies between 1 and 450 MeV were described in ref. 90 (ed. note).

2)Here ^{1}E represents the singlet even-parity state. The singlet odd-parity, triplet even-parity, and triplet odd-parity states are ^{1}O, ^{3}E, and ^{3}O, respectively.

3)Transitions in which the second nucleon (not in a pion−nucleon subsystem) is in S, P, and D states with respect to the center of mass of the entire system are also called "pion production with, respectively, S, P, and D separation of the final system" (ed. note).

4)Absorption in the initial ^{3}S states was neglected in the Mandelstam model.[3] The need for inclusion of this absorption is discussed at the end of this section.

5)Production in the D state is neglected in the Mandelstam model.[3]

6)R. Ya. Zul'karnev et al. recently performed new measurements of the angular dependences of the asymmetry[91] and the depolarization[92] in elastic p−p scattering at 635 MeV. Yu. M. Kazarinov et al. measured the parameters[93] A and[94] D for elastic p−n scattering near 630 MeV (ed. note).

7)The results of recent phase-shift analyses of p−p scattering at 635 MeV carried out at Dubna were described in refs. 91, 95, and 96 (ed. note).

8)In stating that the phase-shift analysis for p−p scattering near 660 MeV has yielded "unambiguous results," we mean that all the solutions found, at least for the lower-lying states of the p−p system, agree qualitatively with solution 1, found below 400 MeV. The scatter in the values of the phase shifts for the various solutions is due primarily to the incompleteness of the information on meson production and the absence of a reliable method for taking into account inelastic reactions.[97] This scatter is not always accurately reflected in the phase-shift errors calculated from the error matrix[62] (ed. note).

9)Such an analysis was carried out by Vovchenko et al.[96] Four solutions were found; the real parts of the phase shifts for the lower-order partial waves of these solutions correspond (within the scatter characteristic of the solutions found elsewhere[31,46-51]) to solution 1 for energies below 400 MeV (ed. note).

10)See also the corresponding discussion in Sec. 5.

11)Phase-shift analyses of p−p and n−p scattering at[98] 735 MeV and p−p scattering at[99] 1 GeV have been carried out at Dubna. Four solutions were found for 735 MeV, for two of which $\delta(^1S_0) < 0$. The set of phase shifts describing the 1-GeV experimental data was obtained by extrapolating the solution for 630 MeV as part of the planning for the 1 GeV experiments (ed. note).

12)Kazarinov et al.[100] worked out a method for discriminating among statistical hypotheses and used this method to reject one of the two sets possible for 630 MeV (set 1).[61] After meson production from the $^3F_4$ state was taken into account along with the remaining solution (set 2), a new set of phase shifts (set 3) was obtained.[101] The results of the measurements of parameter A in p−n scattering at[93] 605 MeV were used to refine sets 2 and 3. Under the assumption that the elastic part of the amplitude for nucleon−nucleon scattering for L > 5 states can be described in the one-pion approximation and that meson production proceeds from $^3P_{0,1,2}$, $^1D_2$, and $^3F_{2,3,4}$ states, it was shown[93] that set 2 can be discarded on the basis of the τ criterion.[102] This conclusion was recently supported by depolarization measurements in elastic p−n scattering[94] at 612 MeV. In set[93] 3 the phase shift of the $^3D_3$ state becomes negative (ed. note).

13)In refs. 103 and 104 the one-pion-exchange model taking into account the pion form factor of nucleons and the singularity in the amplitude of the S_{11} state of the πN system off the mass shell was used successfully to describe polarization effects in the reactions $pp \rightarrow \pi^+pn$ and $pp \rightarrow \pi^0pp$, even at 669 MeV (ed. note).

14)At present there is only one solution (set 3)[93] at 630 MeV (see footnote 12). From this solution we find $\delta(^3S_1) = -17.40 \pm 5.44°$ (ed. note).

15)Solutions A, B, C, and D for the phase shifts for p−p scattering at 640 MeV, found at Dubna,[96] lead to the following respective interval parameters ρp: 0.4 ± 0.2, −0.2 ± 0.1, −0.2 ± 0.1, and −0.1 ± 0.2, in agreement with the conclusion reached by the author (ed. note).

16)The effects of incorporating one-boson exchange in NN interactions were also discussed in refs. 105-108 (ed. note).

17)Correspondingly, in the translation of this paper into Russian, solutions[61] KLPJ-1,2 and[50] K-Sh for 630 MeV were replaced in Tables 3-5 by the more recent solutions BGKK-II and III;[93] in addition, solution A from ref. 96 was added to Table 3 (ed. note).

1. N. Hoshizaki and S. Machida, Progr. Theor. Phys., 29, 44 (1963).
2. N. Hoshizaki and S. Machida, Progr. Theor. Phys., 29, 49 (1963).
3. S. Mandelstam, Proc. Roy. Soc., A244, 491 (1958).
4. N. Hoshizaki, Prog. Theor. Phys., 29, 321 (1963).
5. Y. Hama and N. Hoshizaki, Prog. Theor. Phys., 31, 615, 1162 (1964).

[6]R. Ya. Zhul'karneev and I. N. Silin, Phys. Lett., 3, 265 (1963); Zh. Eksp. Teor. Fiz., 45, 664 (1963) [Sov. Phys.-JETP, 18, 456 (1964)].
[7]Y. Hama and N. Hoshizaki, Prog. Theor. Phys., 34, 584 (1965).
[8]The one-boson-exchange model was reviewed in detail by S. Ogawa et al. in Progr. Theor. Phys., Suppl., No. 39, 140 (1967).
[9]Y. Hama, Prog. Theor. Phys., 35, 261 (1966).
[10]U. Amaldi, Jr., R. Biancastelli, and S. Francaviglia, Nuovo Cimento, 47, 85 (1967).
[11]N. Hoshizaki, Rev. Mod. Phys., 39, 700 (1967).
[12]R. A. Arndt, Rev. Mod. Phys., 39, 710 (1967).
[13]Y. Higuchi and S. Machida, Progr. Theor. Phys., 36, 313 (1966).
[13a]M. Hama and M. Kawaguchi, Progr. Theor. Phys., 36, 1154 (1966).
[14]M. Taketani, S. Nakamura, and M. Sasaki, Progr. Theor. Phys., 6, 581 (1951).
[15]J. Iwadare et al., Progr. Theor. Phys., Suppl., No. 3, 32 (1956).
[16]P. Cziffra et al., Phys. Rev., 114, 880 (1959); 116, 1248 (1959).
[17]R. Jastrow, Phys. Rev., 81, 165 (1951).
[18]O. Chamberlain et al., Phys. Rev., 105, 288 (1957); H. P. Stapp, T. J. Ypsilantis, and N. Metropolis, Phys. Rev., 105, 302 (1957).
[19]T. Hamada and I. D. Johnston, Nucl. Phys., 34, 382 (1962).
[20]J. K. Perring, Nucl. Phys., 42, 306 (1963); P. Signell and D. L. Marker, Phys. Rev., 134, B365 (1964); P. Signell, Phys. Rev., 135, B1344 (1964).
[21]K. Nishimura, Prog. Theor. Phys., Suppl., No. 39, 286 (1967).
[22]M. H. MacGregor and R. A. Arndt, Phys. Rev., 139, B362 (1965).
[23]G. Breit et al., Phys. Rev., 120, 2227 (1960); M. H. Hull et al., Phys. Rev., 122, 1606 (1961).
[24]H. P. Stapp, H. P. Noyes, and M. J. Moravcsik, Proceedings of the 1960 International Conference on High-Energy Physics, Rochester, New York (1960), p. 128; Proceedings of the 1962 International Conference on High-Energy Physics, CERN, Geneva (1962), p. 131.
[25]M. H. MacGregor, R. A. Arndt, and R. M. Wright, Phys. Rev., 169, 1128 (1968).
[26]R. Tamagaki and W. Watari, Prog. Theor. Phys. Suppl., No. 39, 23 (1967).
[27]N. Hoshizaki et al., Prog. Theor. Phys., 27, 1199 (1962).
[28]S. Sawada et al., Prog. Theor. Phys., 28, 991 (1962).
[29]S. Sawada et al., Prog. Theor. Phys., 32, 380 (1964).
[30]L. M. Soroko, Zh. Eksp. Teor. Fiz., 35, 276 (1958) [Sov. Phys.-JETP, 8, 190 (1959)].
[31]L. S. Azhgirei, N. P. Klepikov, Yu. P. Kumekin, M. G. Meshcheryakov, S. B. Nurushev, and G. D. Stoletov, Phys. Lett., 6, 196 (1963); Zh. Eksp. Teor. Fiz., 45, 1174 (1963) [Sov. Phys.-JETP, 18, 810 (1964)].
[32]Y. Hama and N. Hoshizaki, Prog. Theor. Phys., 31, 609 (1964).
[33]Yu. M. Kazarinov and Yu. N. Simonov, Yad. Fiz., 4, 139 (1966).
[34]J. G. Rushbrooke et al., Nuovo Cimento, 33, 1509 (1964).
[35]V. Guzhavin et al., Zh. Eksp. Teor. Fiz., 46, 1245 (1964) [Sov. Phys.-JETP, 19, 847 (1964)].
[36]K. S. Marish and L. M. Soroko, Zh. Eksp. Teor. Fiz., 40, 605 (1961) [Sov. Phys.-JETP, 13, 423 (1961)].
[37]V. G. Vovchenko, Yad. Fiz., 3, 1101 (1966) [Sov. J. Nucl. Phys., 3, 803 (1966)].
[38]A. P. Batson et al., Proc. Roy. Soc., A251, 218 (1959).
[39]Cross-section data are reported by W. N. Hess in: Rev. Mod. Phys., 30, 368 (1958) (a review of data obtained up to 1958); V. Guzhavin et al., Zh. Eksp. Teor. Fiz., 47, 1228 (1964) [Sov. Phys.-JETP, 20, 830 (1965)].
[40]Polarization data are reported by M. G. Meshcheryakov, S. B. Nurushev, and G. D. Stoletov, Zh. Eksp. Teor. Fiz., 33, 37 (1957) [Sov. Phys.-JETP, 6, 28 (1958)]; L. S. Azhgirei et al., Yad. Fiz., 2, 892 (1965) [Sov. J. Nucl. Phys., 2, 636 (1966); Phys. Lett., 18, 203 (1965).
[41]Depolarization data are reported by Yu. P. Kumekin et al., Zh. Eksp. Teor. Fiz., 38, 1451 (1960) [Sov. Phys.-JETP, 11, 1049 (1060)].
[42]Data on the parameter C_{nn} are reported by B. M. Golovin et al., Zh. Eksp. Teor. Fiz., 41, 83 (1961); 44, 142 (1963) [Sov. Phys.-JETP, 14, 63 (1962); 17, 98 (1963)].
[43]Data on the parameter C_{kp} are reported by V. I. Nikanorov et al., Zh. Eksp. Teor. Fiz., 42, 1209 (1962) [Sov. Phys.-JETP, 15, 837 (1962)].
[44]Data on the parameter R are reported by Yu. P. Kumekin et al., Zh. Eksp. Teor. Fiz., 43, 1665 (1962) [Sov. Phys.-JETP, 16, 1175 (1963)].
[45]Data on the parameter A are reported by Yu. P. Kumekin et al., Zh. Eksp. Teor. Fiz., 46, 50 (1964) [Sov. Phys.-JETP, 19, 36 (1964)].
[46]I. Bystritskii and R. Ya. Zul'karneev, Zh. Eksp. Teor. Fiz., 45, 1169 (1963) [Sov. Phys.-JETP, 18, 806 (1964)].
[47]L. S. Azhgirei et al., Zh. Eksp. Teor. Fiz., 46, 1074 (1964) [Sov. Phys.-JETP, 19, 728 (1964)].
[48]L. S. Azhgirei et al., Yad. Fiz., 2, 892 (1965) [Sov. J. Nucl. Phys., 2, 636 (1966)].
[49]L. S. Azhgirei, Yad. Fiz., 4, 1248 (1966) [Sov. J. Nucl. Phys., 4, 896 (1967)].
[50]Yu. M. Kazarinov, Rev. Mod. Phys., 39, 706 (1967).
[50a]B. M. Golovin et al., Yad. Fiz., 6, 804 (1967) [Sov. J. Nucl. Phys., 6, 585 (1968)].
[51]M. H. MacGregor, R. A. Arndt, and R. M. Wright, Phys. Rev., 169, 1149 (1968).
[52]N. Hoshizaki and S. Machida, Prog. Theor. Phys., 30, 575 (1963).
[53]L. S. Azhgirei, Zh. Eksp. Teor. Fiz., 45, 1988 (1963) [Sov. Phys.-JETP, 18, 1365 (1964)]; Yad. Fiz., 1, 876 (1965) [Sov. J. Nucl. Phys., 1, 627 (1965)].
[54]R. Roth et al., Phys. Rev., 140, B1533 (1965).
[54a]P. Limon et al., Phys. Rev., 169, 1026 (1968).
[55]Z. Janout, Yu. M. Kazarinov, and F. Lehar, Report No. E-2743, Dubna (1966).
[56]Data on pion production are reported by V. E. Barnes et al., Phys. Rev. Lett., 7, 288 (1961).
[57]Data on the differential cross section are reported by W. K. McFarlane et al., Nuovo Cimento, 28, 943 (1963); Dowell et al., Nuovo Cimento, 18, 818 (1960); Phys. Lett., 12, 252 (1964).
[58]Data on polarization are reported by Homer et al., Nuovo Cimento, 23, 690 (1962).
[59]Data on polarization and Cnn are reported by Cozzika et al., Phys. Rev., 164, 1672 (1967).
[59a]N. Hoshizaki and T. Katoda, Prog. Theor. Phys., 42, 815, 826 (1969).
[60]Yu. M. Kazarinov and V. S. Kiselev, Zh. Eksp. Teor. Fiz., 46, 797 (1964) [Sov. Phys.-JETP, 19, 542 (1964)].
[61]Yu. M. Kazarinov et al., Yad. Fiz., 4, 567 (1966); 5, 140 (1967) [Sov. J. Nucl. Phys., 4, 402 (1967); 5, 97 (1967)].
[62]M. H. MacGregor, R. A. Arndt, and R. M. Wright, UCRL-70075 (Part IX) (1968).
[63]E. Ferrari and F. Selleri, Nuovo Cimento, 21, 1020 (1961); Nuovo Cimento, Supp., No. 24, 453 (1962).
[64]U. Amaldi, Jr., Rev. Mod. Phys., 39, 649 (1967).
[65]S. Francaviglia, Prog. Theor. Phys., 39, 676 (1968).
[66]See also Sec. 6 of ref. 8.
[67]N. Levinson, Kgl. Danske Vid. Selskab. Mat.-Fys. Medd., 25, No. 9 (1949).
[68]Y. Hama and N. Hoshizaki, Prog. Theor. Phys., 34, 455 (1965).
[69]J. M. Jauch, Helv. Phys. Acta, 30, 143 (1957); M. Ida, Prog. Theor. Phys., 21, 625 (1959); M. T. Vaughn, R. Aaron, and R. D. Amado, Phys. Rev., 124, 1258 (1961).
[69a]J. B. Hartle and C. E. Jones, Ann. Phys. (New York), 38, 348 (1966).
[70]M. Taketani, S. Machida, and S. Onuma, Prog. Theor. Phys., 6, 638 (1951).
[71]B. Cork, W. A. Wenzel, and C. W. Causey, Phys. Rev., 107, 859 (1957).
[72]Fujii et al., Phys. Rev., 128, 1836 (1962); W. J. Fickinger et al., Phys. Rev., 125, 2082 (1962).
[73]Bareyre et al., Nuovo Cimento, 20, 1049 (1961).
[74]H. A. Neal and M. J. Longo, Phys. Rev., 161, 1374 (1967).
[75]Data on the differential cross section for elastic scattering are reported by W. M. Preston, R. Wilson, and J. C. Street, Phys. Rev., 118, 579 (1960); Smith et al., Phys. Rev., 123, 2160 (1961); Fujii et al., Phys. Rev., 128, 1836 (1962), Melissions et al., Phys. Rev., 128, 2373 (1962); S. A. Azimov et al., Zh. Eksp. Teor. Fiz., 42, 430 (1962) [Sov. Phys.-JETP, 15, 299 (1962)]. Data on the cross section for inelastic scattering are reported by Fowler et al., Phys. Rev., 103, 1480 (1956); M. J. Longo and B. J. Moyer, Phys. Rev., 125, 701 (1962). Data on polarization are reported by Grannis et al., Phys. Rev., 148, 1297 (1966).
[76]R. Tamagaki, Prog. Theor. Phys., 39, 91 (1968); also private communication.
[77]S. Otsuki, R. Tamagaki, and M. Wada, Prog. Theor. Phys., 32, 220 (1964).
[78]S. Machida, Prog. Theor. Phys., Suppl., No. 39, 91 (1967), Ch. 2.
[79]R. Tamagaki, M. Wada, and W. Watari, Prog. Theor. Phys., 31, 623 (1964); see also Sec. 4 of ref. 26.
[80]G. F. Chew, private communication.
[80a]R. D. Tripp, Proceedings of the Enrico Fermi International School of Physics, Vol. 33 (1963), p. 70.

[81]Borghini et al., Phys. Lett., 24B, 77 (1967).
[82]Bellettini, et al., Phys. Lett., 14, 164 (1965).
[83]K. J. Foley et al., Phys. Rev. Lett., 14, 74 (1965).
[84]J. Orear, Phys. Lett., 13, 190 (1964).
[85]M. Taketani, Prog. Theor. Phys. Suppl, No. 39, 1 (1967).
[86]S. Otsuki, Prog. Theor. Phys. Suppl, No. 42, 39 (1968).
[87]L. I. Lapidus, Zh. Eksp. Teor. Fiz., 34, 1148 (1958) [Sov. Phys. – JETP, 7, 794 (1958)].
[88]See also the appendix in ref. 77.
[89]N. Hoshizaki, Prog. Theor. Phys. Suppl, No. 42, 107 (1968).
[90]M. H. MacGregor, R. A. Arndt, and R. M. Wright, Phys. Rev., 182, 1714 (1969).
[91]R. Ya. Zul'karneev et al., Yad. Fiz., 6, 995 (1967) [Sov. J. Nucl. Phys., 6, 725 (1968)].
[92]R. Ya. Zul'karneev, V. S. Nadezhdin, and V. I. Satarov, Yad. Fiz., 11, 178 (1970) [Sov. J. Nucl. Phys., 11, 98 (1970)].
[93]S. I. Bilen'kaya et al., Zh. Eksp. Teor. Fiz., 59, 1049 (1970) [Sov. Phys. – JETP, 32, 569 (1971)].
[94]L. N. Glonti, Yu. M. Kazarinov, and M. R. Khayatov, Preprint R1-5743, JINR, Dubna (1971).
[95]R. Ya. Zul'karneev et al., Preprint R1-4155, JINR, Dubna (1968).
[96]V. G. Vovchenko R. Ya. Zul'karneev, and V. S. Kiselev, Zh. Eksp. Teor. Fiz., 58, 825 (1970) [Sov. Phys. – JETP, 31, 442 (1970)].
[97]M. H. MacGregor, Proceedings of the First International Conference on N – N and π – N interactions [Russian translation], R1-3951, Dubna (1968), p. 95.
[98]S. I. Bilen'kaya et al., Nucl. Phys., B13, 375 (1969).
[99]L. N. Glonti et al., Preprint R1-5737, JINR, Dubna (1971).
[100]Yu. M. Kazarinov et al., Yad. Fiz., 7, 340 (1968) [Sov. J. Nucl. Phys., 7, 245 (1968)].
[101]L. N. Glonti et. al, Yad. Fiz., 7, 1060 (1968) [Sov. J. Nucl. Phys., 7, 637 (1968)].
[102]A. Pazman, Preprint E5-3775, JINR, Dubna (1968); A. Pazman et al., J. Phys., B19, 882 (1969).
[103]L. S. Azhgirei and V. I. Chizhikov, Preprint R2-4937, JINR, Dubna (1970).
[104]L. S. Azhgirei et al., Yad. Fiz., 13, 581 (1971) [Sov. J. Nucl. Phys., 13, 328 (1971)].
[105]L. S. Azhgirei and V. I. Chizhikov, Preprint R-2584, JINR, Dubna (1966).
[106]L. S. Azhgirei and V. I. Chizhikov, Yad. Fiz., 5, 405 (1967) [Sov. J. Nucl. Phys., 5, 284 (1967)].
[107]L. S. Azhgirei and V. I. Chizhikov, Preprint R2-3188, JINR, Dubna (1967).
[108]L. S. Azhgirei and V. I. Chizhikov, Preprint E1-3420, JINR, Dubna (1967).